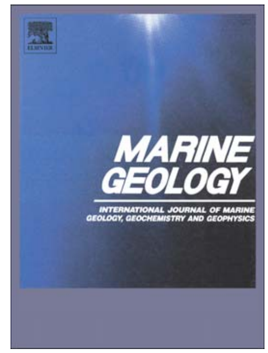

Ice-sheet grounding-zone wedges (GZWs) on high-latitude continental margins

C.L. Batchelor, J.A. Dowdeswell

PII: S0025-3227(15)00030-4
DOI: doi: 10.1016/j.margeo.2015.02.001
Reference: MARGO 5256

To appear in: *Marine Geology*

Received date: 31 July 2014
Revised date: 3 February 2015
Accepted date: 6 February 2015

Ice-sheet grounding-zone wedges (GZWs) on high-latitude continental margins

C.L. Batchelor[1], J.A. Dowdeswell[1]

[1] *Scott Polar Research Institute, University of Cambridge, Cambridge CB2 1ER, UK*

Corresponding author: Christine Batchelor, clb70@cam.ac.uk, 01223 336540

Keywords: grounding-zone wedges; palaeo-ice streams; cross-shelf troughs; seismic reflection; pinning points; ice shelves

ABSTRACT

Grounding-zone wedges (GZWs) are asymmetric sedimentary depocentres which form through the rapid accumulation of glacigenic debris along a line-source at the grounding zone of marine-terminating ice sheets during still-stands in ice-sheet retreat. GZWs form largely through the delivery of deforming subglacial sediments. The presence of GZWs in the geological record indicates an episodic style of ice retreat punctuated by still-stands in grounding-zone position. Moraine ridges and ice-proximal fans may also build up at the grounding zone during still-stands of the ice margin, but these require either considerable vertical accommodation space or sediment derived from point-sourced subglacial meltwater streams. By contrast, GZWs form mainly where floating ice shelves constrain vertical accommodation space immediately beyond the grounding-zone. An inventory of GZWs is compiled from available studies of bathymetric and acoustic data from high-latitude continental margins. The locations and dimensions of GZWs from the Arctic and Antarctic, alongside a synthesis of their key architectural and geomorphic characteristics, is presented. GZWs are only observed within cross-shelf troughs and major fjord systems, which are the former locations of ice streams and fast-flowing outlet glaciers. Typical high-latitude GZWs are less than 15 km in along-flow direction and 15 to 100 m thick. GZWs possess a transparent to chaotic acoustic character, which reflects the delivery of diamictic subglacial debris. Many GZWs contain seaward-dipping reflections, which indicate sediment progradation and wedge-growth through continued delivery of basal sediments. GZW formation is inferred to require high rates of sediment delivery to a fast-flowing ice margin that is relatively stable for probably decades to centuries. Although the long-term stability of the grounding zone is controlled by ice-sheet mass balance, the precise location of any still-stands is influenced strongly by the geometry of the continental shelf. The majority of high-latitude GZWs occur at vertical or lateral pinning points, which encourage grounding-zone stabilisation through increasing basal and lateral drag and reducing mass flow across the grounding zone.

1. INTRODUCTION

The grounding zone of marine-terminating ice sheets is the transitional zone at which the ice-sheet base ceases to be in contact with the underlying substrate. Marine-terminating glaciers can be categorised into those with ice-shelf margins, in which floating ice extends a few to several hundreds of kilometres offshore from the grounding zone (Fig. 1A), and those with tidewater margins that lack floating ice beyond the grounding zone (Fig. 1B). At ice-shelf margins, a water-filled cavity, which is shallow close to the grounding zone and can be up to several hundred metres in depth further offshore, extends from the grounding zone to the calving front of the floating ice shelf (Fig. 1A). The grounding zone of a tidewater glacier occurs at approximately the same position at which iceberg calving takes place (Fig. 1B).

The grounding zone of ice sheets has been referred to previously as the grounding line (e.g. Powell, 1991; Powell and Domack, 1995; Powell and Alley, 1997; Alley et al., 2007). However, we consider the term grounding zone to be more appropriate as it reflects the temporally variable nature of the location at which the ice loses contact with the sea floor. The precise location of ice-sheet grounding is affected by short-term variations in forcing factors such as tides, as well as climatically-induced variations in thinning and rates of mass loss (Bindschadler et al., 2003; Gudmundsson, 2007; Murray et al., 2007).

The grounding zone is a key site at which ice and meltwater are transferred from the ice sheet to the marine environment (Powell et al., 1996; Christianson et al., 2013; Horgan et al., 2013). It is a line-source and can extend for tens to hundreds of kilometres in lateral width. Mass is lost from marine-terminating glaciers through iceberg calving, meltwater runoff, and melting from tidewater ice cliffs or the ice-shelf base (e.g. Jenkins and Doake, 1991; Rignot and Jacobs, 2002; Enderlin and Howat, 2013). Marine-terminating glaciers, which are close to floatation for long distances inshore of the grounding zone, therefore generally respond more sensitively to climatically-induced changes in ice thickness and sea level compared with their land-terminating counterparts, which lose mass predominantly through meltwater runoff (Alley et al., 2007). In areas where fast-flowing ice streams are present, the marine ice-sheet margin is a major focus for the delivery of icebergs and freshwater into the ocean. Marine-terminating ice streams in Greenland and Antarctica are currently responsible for the majority of mass loss from these ice sheets (Rignot and Kanagaratnam, 2006; Shepherd and Wingham, 2007; Rignot et al., 2008; Pritchard et al., 2009). Palaeo-ice streams exerted a major influence on ice-sheet behaviour and had the potential to cause abrupt climatic change through the rapid delivery of ice and freshwater to the ocean (Overpeck et al., 1989; Bond et al., 1992; Stokes et al., 2005).

The grounding zone of marine-terminating ice sheets is also a site at which sediment is transferred from the ice sheet to the marine environment. Diamictic subglacial till can be emplaced directly at the grounding zone from deforming sedimentary beds beneath fast-flowing ice streams (Alley et al., 1986, 1989; Anandakrishnan et al., 2007). Multiple sheet-like deposits of acoustically chaotic to transparent subglacial till, separated by erosional unconformities, can build up within fjords and on continental shelves over successive ice advances (Fig. 1C and D) (e.g. Larter and Barker, 1989; King, 1993; Rise et al., 2005). During full-glacial periods of ice-sheet expansion relative to today, ice sheets supply subglacial till directly to the continental shelf break; this debris is often remobilised subsequently by mass-wasting processes on the upper-slope (Fig. 1C and D) (Alley et al., 1989; Dowdeswell et al., 1996; Laberg et al., 2000; Taylor et al., 2002; Nygård et al., 2005). Large sedimentary depocentres or trough-mouth fans build up on the slope over successive glaciations as a result of the rapid delivery of deformable sediment to the shelf edge by fast-flowing ice streams (Fig. 1C) (Vorren et al., 1998; Dowdeswell and Siegert, 1999).

In addition to being emplaced subglacially, sediment can also be transferred across the grounding zone through subglacial or englacial meltwater channels, which provide point sources of sorted sediment to the marine environment (Powell, 1990; Mugford and Dowdeswell, 2011; Dowdeswell et al., In Press). A component of sedimentation may also occur through the melt-out of subglacial debris from ice at or immediately beyond the grounding zone (Alley et al., 2007). The coarse fraction of the sediment that is released from basal melting at the grounding zone and beneath ice shelves forms marine sediment units composed of mud, sand, gravel and till pellets, whereas the fine fraction forms a sedimentary drape through the rain-out of particles transported in suspension by currents (Domack et al., 1999; Evans and Pudsey, 2002; Christoffersen et al., 2010; Kilfeather et al., 2011).

Providing there is space for sediment accumulation, discrete sedimentary depocentres, including grounding-zone wedges (GZWs), moraine ridges and ice-proximal fans, will build up during still-stands or re-advances of the grounding zone. The identification of these depocentres in the geological record can provide information about the dynamics of former ice sheets and the locations of still-stands or re-advances of the grounding zone (e.g. Shipp et al., 1999; Mosola and Anderson, 2006; Ottesen et al., 2007; Dowdeswell et al., 2008).

The existence of wedge-shaped depocentres, formed by sediment progradation at the grounding zone of former ice streams, was first hypothesised on the basis of the likely high till flux implied by the discovery of a 6 m-thick layer of deforming till beneath the Whillans Ice Stream (formerly Ice Stream B) in West Antarctica (Blankenship et al., 1987; Alley et al., 1987, 1989). Since GZWs were first identified in the 1990’s (Anderson and Bartek, 1992; Powell and Domack, 1995; Anderson, 1997; Bart and Anderson, 1997; Powell and Alley, 1997; O’Brien et al., 1999), a large number of GZWs has been described from high-latitude cross-shelf troughs in both hemispheres (e.g. Ó Cofaigh et al., 2005a; Evans et al., 2006; Mosola and Anderson, 2006; Ottesen et al., 2007, 2008; Rydningen et al., 2013). However, a synthesis of their locations, morphological and stratigraphical characteristics is currently lacking. There is also still some uncertainty as to what differentiates GZWs from other glacier-influenced sedimentary depocentres, such as submarine moraines and till tongues (Powell, 1981; King et al., 1991).

In this paper, we present an inventory of GZWs which is compiled from available studies of bathymetric, shallow-acoustic and seismic data from high-latitude continental margins. Here, GZWs are defined as wedge-shaped deposits composed predominantly of glacial diamict or till, which are formed by high rates of sediment delivery to the grounding zone of fast-flowing ice streams during still-stands in ice retreat (Ottesen et al., 2007; Dowdeswell et al., 2008; Dowdeswell and Fugelli, 2012).

We present the locations of 143 GZWs from the high-latitude continental shelves of Antarctica, Greenland, Norway, Canada and the Barents Sea, alongside a synthesis of their key sedimentary, architectural and geomorphic characteristics. In this study, many of the high-latitude GZWs are categorised into one or more of four 'types' based on their position within cross-shelf troughs or fjords: at shallow vertical pinning points in the underlying bathymetry; at narrow lateral pinning points; on the outermost continental shelf; and at the outer-shelf lateral margins of former ice streams. Controls on GZW formation are considered in relation to cross-shelf trough geometry, climatic changes and ice-sheet internal dynamics.

2. BACKGROUND: ICE-MARGINAL DEPOCENTRES AND OTHER LANDFORMS PRODUCED AT THE GROUNDING ZONE OF MARINE-TERMINATING ICE SHEETS

2.1 GZWs

GZWs form mainly through subglacial deposition of deforming till at the grounding zone, which may then be redistributed by gravity-flow processes to produce wedge-shaped deposits (King et al., 1991; Powell and Alley, 1997; Dowdeswell and Fugelli, 2012). GZWs typically possess a semi-transparent to chaotic acoustic character, which reflects the delivery of diamictic subglacial debris (Alley et al., 1989; Ó Cofaigh et al., 2005b; Dowdeswell and Fugelli, 2012; Andreassen et al., 2014), and are asymmetric in the direction of former ice-flow, with steeper ice-distal sides (Fig. 2A). GZW dimensions are controlled by the flux of sediment to the grounding zone, the shape of the sub-ice cavity (Fig. 1A), the width of the palaeo-ice stream, and the duration of the still-stand during longer-term ice retreat (Alley et al., 2007; Dowdeswell and Fugelli, 2012). If sediment flux across the grounding zone is known, GZW volume can be used to estimate the duration of an ice margin still-stand, which is typically decades to centuries (Larter and Vanneste, 1995; Alley et al., 2007; Anandakrishnan et al., 2007; Dowdeswell et al., 2008; Livingstone et al., 2012). Recent attempts to drill through GZWs aimed to reveal the precise timing and duration of stills-stands of the grounding zone (Hanebuth et al., 2014).

GZWs are formed by the build-up of sediments delivered at relatively high rates to the grounding zone (Fig. 1C). The continuation of fast, ice-streaming flow during the final phase of GZW formation has been inferred from the identification of mega-scale glacial lineations (MSGL), which are indicative of fast ice flow, overprinting GZWs in a number of locations (e.g. Fig. 2A) (Ó Cofaigh et al., 2005a; Ottesen et al., 2008; Graham et al., 2010). The presence of GZWs in the geological record indicates episodic palaeo-ice-stream retreat punctuated by still-stands in the grounding-zone position (Dowdeswell et al., 2008; Ó Cofaigh et al., 2008).

The term GZW has emerged from an assortment of nomenclature to describe accumulations of sediment produced along line-sources at the grounding zone (Table 1), including ‘till tongues’ (King and Fader, 1986; Dreimanis, 1987; King et al., 1987, 1991) and ‘till deltas’ **(**Bentley et al., 1988; Alley et al., 1989; Schever, 1991). Till tongues are composed of till deposited during ice-sheet advances across the continental shelf, inter-fingered with glacimarine sediments (King et al., 1991). Till tongues may contain sediment that was originally deposited within a GZW, but has been partially eroded and redistributed by a subsequent ice advance. In this study, till tongues, which possess a sheet-like geometry in seismic records (King, 1980; King and Fader, 1986; King et al., 1987, 1991), are considered to be distinct from positive-relief landforms, such as moraines and GZWs.

The term till delta has been used previously to describe wedge-shaped accumulations of glacigenic debris on the continental shelf (Alley et al., 1987, 1989; Larter and Vanneste, 1995). In order to avoid defining all the sediment as till, and to remove any association with sea level, the term GZW has now generally encompassed and replaced the term till delta (Table 1) (Powell and Domack, 1995; Powell and Alley, 1997; Shipp et al., 2002; Anandakrishnan et al., 2007; Livingstone et al., 2012).

We now discuss how GZWs can be differentiated from other ice-marginal landforms produced at the grounding zone of marine-terminating ice sheets, including submarine moraines and ice-proximal fans (Fig. 2).

2.2 Moraines

Submarine transverse moraines can be categorised into large terminal and recessional moraine ridges, hummocky-terrain belts and small retreat moraines (Fig. 2B to D).

2.2.1 Large terminal/ recessional moraines

Large terminal and recessional moraine ridges are typically several tens of metres thick and less than 2 km wide in the former ice-flow direction (e.g. Sexton et al., 1992; Seramur et al., 1997; Ottesen and Dowdeswell, 2006, 2009; Ottesen et al., 2007). Although these moraines can possess similar thicknesses to GZWs, they have clear positive relief and lower length-to-height ratios (typically less than 10:1) compared with the more subdued and wedge-like forms of GZWs (Fig. 2A and B) (Dowdeswell and Fugelli, 2012). This suggests that, unlike GZWs, moraine ridges are not constrained by the roof of a sub-ice shelf cavity (Fig. 1A), and are probably formed mainly at tidewater ice cliffs (Fig. 1B).

Submarine moraines form through a combination of processes, including meltwater deposition, melt-out of basal and englacial debris, squeeze-push processes from under the ice mass, lodgement and sediment deformation (Powell, 1981; Smith, 1990; Powell and Domack, 1995; Powell and Alley, 1997). Moraines are typically composed of various unsorted ice-contact sediments and therefore possess a semi-transparent to chaotic character on acoustic profiles (e.g. Stoker and Holmes, 1991; Sexton et al., 1992; King, 1993; Shaw, 2003).

Whereas GZWs are formed by high rates of sediment delivery to the grounding zone, large moraine ridges are more typically observed in shallow, inter-ice stream areas of high-latitude continental shelves, where they record the former extent of relatively slow-moving ice (Fig. 1D) (Dahlgren et al., 2002b; Dowdeswell and Elverhøi, 2002; Landvik et al., 2005; Ottesen and Dowdeswell, 2009; Klages et al., 2013). A number of large terminal-moraine ridges have been described from inter-trough regions of the Svalbard and Norwegian continental shelves; these landforms are interpreted to delimit the maximum extent of the Barents-Kara and Scandinavian ice sheets during the last glacial maximum (e.g. Dahlgren et al., 2002b; Vorren and Plassen, 2002; Ottesen et al., 2005a, 2007, 2008; Rydningen et al., 2013). Large recessional-moraine ridges, which record the position of still-stands in the grounding zone during deglaciation, have also been described from high-latitude continental shelves and fjords (Elverhøi et al., 1983; Syvitski, 1989; Cai et al., 1997; Powell and Domack 2002; Landvik et al., 2005; Hodgson et al., 2014). Arcuate moraine ridges often develop at the mouths of fjords, which act as lateral pinning points for stabilisation of the grounding zone during retreat (Fig. 1D) (Dowdeswell et al., 1994; Shaw, 2003; Ottesen et al., 2007; Ottesen and Dowdeswell, 2009; Shaw et al., 2009; Dowdeswell and Vasquez, 2013).

Although terminal moraines are typically formed on inter-ice stream areas of a continental margin, which are characterised by relatively low full-glacial sedimentation rates (Elverhoi et al., 1998), the Skjoldryggen moraine ridge on the mid-Norwegian shelf is located at the shelf break in a region which has experienced high rates of sediment delivery during the last three glaciations (Rise et al., 2005). This moraine has, however, been interpreted to have formed at times when fast ice flow and rapid sediment delivery may have ceased (Ottesen et al., 2005a). Arcuate ridges, interpreted as submarine moraine banks formed during deglaciation of the last British-Irish Ice Sheet, have also been described from cross-shelf troughs on the continental shelf off Britain and Ireland (Bradwell et al., 2008; Dunlop et al., 2010; Clark et al., 2012; Ó Cofaigh et al., 2012).

2.2.2 Hummocky-terrain belts

Submarine hummocky-terrain belts are characterised by irregular assortments of hummocks, ridges and depressions (Fig. 2C), and are formed by uneven sediment deposition and redistribution close to the ice margin (Sharp, 1985; Bennett and Boulton, 1993). In the marine record, hummocky-terrain belts 1 km long and with ridge-amplitudes of around 5 metres have been described from inter-trough regions of the shelf break off northwest Svalbard and northern Norway (Ottesen and Dowdeswell, 2009; Elvenes and Dowdeswell, In Press). Hummocky moraine can be formed by a variety of processes, including sediment lodgement and deformation, glacitectonics and debris accumulation at an active ice margin, and deposition in contact with stagnant ice (Benn and Evans, 2010). Hummocky moraine is sometimes associated with rectilinear networks of crevasse-fill ridges, which are interpreted to be produced by changes in ice buoyancy and the moulding or squeezing upward of deformable sediments into basal crevasses at a grounded ice-sheet margin (Sharp, 1985; Ottesen and Dowdeswell, 2009).

2.2.3 Small retreat moraines

Small retreat moraines typically just a few metres high, which are often referred to as De Geer moraines (Lindén and Möller, 2005), are formed by the delivery of sediment to the glacier or ice-sheet grounding zone during minor ice-margin still-stands or oscillations during overall retreat of a grounded ice mass (Nygård et al., 2004; Ottesen et al., 2005a, 2007; Todd et al., 2007; Dowdeswell et al., 2008; Ottesen and Dowdeswell, 2009). These sedimentary ridges are typically less than 15 m thick and less than 300 m wide (Fig. 2D) (Boulton, 1986; Shipp et al., 2002; Ottesen and Dowdeswell, 2006; Ottesen et al., 2007; Todd et al., 2007; Dowdeswell et al., 2008; Shaw et al., 2009). Small moraine ridges possess sediment volumes that are one or two orders of magnitude less than large terminal moraines or GZWs; this suggests that small moraine ridges record relatively short pauses in the position of the ice margin during deglaciation (Nygård et al., 2004; Ottesen and Dowdeswell, 2006; Ottesen et al., 2007). Small retreat moraines are almost always identified in assemblages containing tens to hundreds of parallel to sub-parallel ridges, rather than as isolated landforms (Figs. 1D and 2D). They are typically evenly spaced, with distances of a few tens to hundreds of metres between ridges (e.g. Boulton, 1986; Shipp et al., 2002; Ottesen and Dowdeswell, 2006; Ottesen et al., 2007; Shaw et al., 2009; Livingstone et al., 2012).

Small moraine ridges are interpreted to be formed by ice pushing of sediment, including folding, faulting and thrusting, during minor ice-sheet re-advances within overall retreat (Solheim and Pfirman, 1985; Hagen, 1987; Boulton et al., 1996; Shipp et al., 2002; Ottesen and Dowdeswell, 2006, 2009). These moraines are often formed annually, with the number of ridges approximating the years over which retreat took place (Boulton, 1986; Ottesen and Dowdeswell, 2006; Dowdeswell et al., 2008). Annual cycles of ice-margin re-advance probably occur as a result of the suppression of iceberg calving by sea-ice buttressing during winter months, which produces minor re-advances superimposed on more general summer retreat (Liestøl, 1976; Boulton, 1986; Ottesen and Dowdeswell, 2006).

Series of small transverse ridges, interpreted as retreat moraines, have been described from shallow inter-ice stream regions of the continental shelf (Ottesen et al., 2005a, 2007; Todd et al., 2007; Ottesen and Dowdeswell, 2009; Shaw et al., 2009), as well as within cross-shelf troughs (Boulton, 1986; Shipp et al., 2002; Mosola and Anderson, 2006; Dowdeswell et al., 2008; Ó Cofaigh et al., 2008; Winkelmann et al., 2010) and high-latitude fjords (Ottesen and

Dowdeswell, 2006; Ottesen et al., 2007). Whereas the presence of GZWs suggests an episodic style of ice-stream retreat, the identification of small retreat moraines overprinting MSGL suggests relatively slow retreat of a grounded marine ice margin, although assessment of this by dated sediment cores is relatively rare (Dowdeswell et al., 2008; Ó Cofaigh et al., 2008).

2.3 Ice-proximal fans

Ice-proximal fans form at the mouths of subglacial meltwater conduits at the grounding zone of a marine-terminating ice mass (Powell, 1984, 1990; Sexton et al., 1992; Powell and Domack, 1995; Seramur et al., 1997; Mugford and Dowdeswell, 2011; Dowdeswell et al., In Press). These landforms, which are sometimes referred to as ice-contact fans (Table 1), are composed of a variety of sediments, including sub-aquatic outwash, gravity flow sediments and suspension settling deposits (Lønne, 1995, 1997; Powell and Alley, 1997). Whereas the geometry of moraine ridges and GZWs suggests sediment delivery along a line-source at the grounding zone (Fig. 2A to D), the fan-shaped geometry of ice-proximal fans is indicative of point-source deposition (Fig. 2E). Where an extensive system of subglacial conduits is present along the grounding zone, individual ice-proximal fans may overlap and become amalgamated into morainal banks (Hunter et al., 1996; Powell and Alley, 1997). Ice-proximal fans are produced during periods of grounding-zone stability and can aggrade to sea level to form ice-contact deltas (Glückert, 1975; Powell, 1990; Smith, 1990; Lønne, 1993; Powell and Domack, 1995).

The formation of ice-proximal fans is dependent on the existence of a channelised meltwater network beneath the ice mass. Ice-proximal fans therefore typically develop in glacial settings where surface-derived meltwater is present (Powell, 1990; Dowdeswell et al., 1998; Siegert and Dowdeswell, 2002). Ice-proximal fans that formed during the last glaciation to present interglacial have been described from the fjords of Alaska, Norway and Svalbard, where they have been observed to accumulate at rates of over 10^6 m^3 per year (Powell, 1990; Lønne, 1995, 1997; Seramur et al., 1997). They are typically up to a few tens of metres thick and up to a few kilometres in length.

The absence of large ice-proximal fans preserved on continental shelves may reflect the highly-variable position of the grounding zone during deglaciation (Dowdeswell et al., In Press). Under 'normal' meltwater discharge conditions, the majority of ice-margin still-stands are probably of insufficient duration to enable the development of large ice-proximal fans. Any fans produced during ice advances are likely to be reworked as they are overrun by the advancing ice mass (Powell, 1990). It is also possible that some ice-proximal fans may have been formed by extreme meltwater discharge events which provided atypically high rates of sediment delivery to the ice margin over a short time-scale during which the grounding zone remained stable (Hirst, 2012; Dowdeswell et al., In Press). Ice-proximal fans are unlikely to form in regions where water flow occurs largely through Darcian processes within deforming basal sediments; they are therefore generally absent from cross-shelf troughs which were the locations of fast-flowing ice streams with deforming beds.

2.4 Controls on ice-marginal landforms produced at the grounding zone

2.4.1 Type of glacier terminus

The nature of the glacier terminus is an important control on the type of depositional landform that is produced at the grounding zone. Tidewater glaciers, which have almost unlimited vertical accommodation space at the grounding zone (Fig. 1B), have been suggested to be associated with the formation of high-amplitude morainal ridges, whereas low-relief GZWs are probably formed preferentially by glaciers with termini ending as floating ice shelves (Fig. 1A) (King and Fader, 1986; King et al., 1987; Powell and Alley, 1997). The low-gradient ice-roofed cavities of ice shelves (Fig. 1A) restrict vertical accommodation space and prevent the aggradation of high-amplitude moraine ridges (Powell, 1990; Dowdeswell and Fugelli, 2012).

2.4.2 Ice velocity and sediment delivery rate

Ice velocity can also control the type of ice-marginal landform produced at the grounding zone. GZWs are produced by rapid grounding-zone sedimentation of deformable debris at fast-flowing ice margins. Where they are identified within cross-shelf troughs, in association with deformable till, MSGL or lateral moraines, GZWs indicate the former presence of ice streams (Fig. 1C) (Dowdeswell et al., 2008; Ottesen and Dowdeswell, 2009). In contrast, terminal moraines appear to be formed mainly at slower-flowing, inter-ice stream margins (Fig. 1D) (Dahlgren et al., 2002a; Dowdeswell and Elverhøi, 2002; Landvik et al., 2005; Ottesen and Dowdeswell, 2009).

2.4.3 Grounding-zone stability

The type and dimensions of an ice-marginal landform is dependent on the duration of still-stands of the grounding zone. GZWs and large terminal-moraine ridges are typically produced during still-stands of at least several decades to centuries, which allow for significant volumes of sediment to build up at a relatively stable grounding zone (Larter and Vanneste, 1995; Alley et al., 2007; Anandakrishnan et al., 2007; Dowdeswell et al., 2008). In contrast, small moraine ridges, which typically possess sediment volumes that are one or two orders of magnitude smaller than terminal-moraine ridges or GZWs, are produced during short-lived still-stands in the grounding zone during overall ice retreat (Nygård et al., 2004; Ottesen et al., 2005a; Dowdeswell et al., 2008; Ottesen and Dowdeswell, 2009).

2.4.4 Subglacial meltwater

The availability of subglacial meltwater has also been proposed as a major control on the formation of ice-proximal landforms (Powell and Alley, 1997; Bjarnadóttir et al., 2013). Moraines have been suggested to form at the margins of temperate or polythermal glaciers where subglacial meltwater is abundant in channelised or sheet flows, whereas GZWs are more likely to be produced at the margins of polythermal or polar ice sheets where deforming beds are present and meltwater is sparser or moving within deforming till by Darcian processes (Powell and Alley, 1997).

Terminal-moraine ridges are widespread within temperate glacier fjords (Powell, 1983; Cai et al., 1997; Dowdeswell and Vasquez, 2013) and on shallow inter-ice stream areas of the continental shelves off Svalbard and Norway (Dahlgren et al., 2002b; Vorren and Plassen, 2002; Ottesen et al., 2005a, 2007, 2008; Rydningen et al., 2013). Very few terminal-moraine ridges have been described from the continental shelves of Greenland and Antarctica (Klages et al., 2013) compared with the large number of GZWs identified in these locations (Larter and Vanneste, 1995; Anderson, 1999; Evans et al., 2005; Mosola and Anderson, 2006; Dowdeswell and Fugelli, 2012; Livingstone et al., 2012). The relative absence of moraine ridges on the shelves of Greenland and Antarctica may reflect a lack of channelised meltwater beneath the former ice sheets. It is also possible that extensive floating ice shelves in these areas precluded the development of high-amplitude moraine ridges. Alternatively, this pattern could be a consequence of the data coverage of these areas, which is generally focused within cross-shelf troughs that were formerly occupied by fast-flowing ice streams. In addition, relatively shallow inter-ice stream banks are often reworked by the ploughing action of iceberg keels making the interpretation of pre-existing landforms difficult (e.g. Dowdeswell et al., 1993, 2014).

Terminal moraines and GZWs have been suggested to represent end-members of a continuum of grounding-zone landforms, reflecting the differing availability of subglacial meltwater (Powell and Alley, 1997). The ice-marginal landforms in Kveithola Trough on the western Barents Sea margin have been proposed to be intermediate forms between GZWs and moraines (Bjarnadóttir et al., 2013). These landforms exhibit the asymmetric geometry and homogeneous fine-grained sediments that are characteristic of GZWs, yet they also contain ice-proximal fans (Fig. 2E) on their ice-distal sides, indicating the former presence of abundant meltwater (Bjarnadóttir et al., 2013). GZWs in climatic settings where ice-sheet mass loss is dominated by meltwater runoff may contain a greater component of sorted sediment derived from subglacial meltwater, compared with GZWs in settings where mass loss is dominated by iceberg calving (Dowdeswell and Fugelli, 2012; Bjarnadóttir et al., 2013).

The formation of ice-proximal fans (Fig. 2E) requires the existence of a channelised meltwater network beneath a marine-terminating ice mass. Ice-proximal fans are therefore commonly observed in temperate glacial regions where surface-derived meltwater is present (e.g. Powell, 1990; Dowdeswell et al., In Press), and are generally lacking from regions in which meltwater is sparser or flows mainly by Darcian processes within deforming basal sediments (Powell, 1990; Powell and Alley, 1997; Siegert and Dowdeswell, 2002).

3. METHODOLOGY

An inventory of high-latitude GZWs is presented in Table 2 and Figures 3 and 4. GZW locations are compiled from available accounts of bathymetric and acoustic data from the high-latitude continental shelves of Canada, Greenland, the Barents Sea, northern Norway and Antarctica (e.g. Anderson, 1997; Domack et al., 1998; Ottesen et al., 2005a, 2008;

Mosola and Anderson, 2006; Rydningen et al., 2013). The approximate locations of the GZWs off northwest and northeast Greenland (Fig. 3C) were determined from newly-available two-dimensional (2-D) seismic reflection data provided by TGS. Due to restrictions on the use of industrial data, the identification numbers of the seismic lines, and details of the acquisition parameters and streamer arrays, are not included. All asymmetric wedges of sediment that are at least 1 km long and 10 m thick were categorised as GZWs.

Our inventory provides data on those landforms on high-latitude margins which have been interpreted as GZWs. However, it is possible that some ice-marginal landforms which fit our criteria to be GZWs may have been omitted from the inventory as a result of their previous classification as moraines, till tongues or till deltas. Our inventory attempts to include GZWs that were originally interpreted as other types of landform before being re-classified as GZWs. For example, the three wedge-shaped landforms in Vestfjorden on the Norwegian margin (nos. 35 to 37 in Table 2 and Fig. 3B), which have been interpreted previously as recessional moraines or till tongues (Ottesen et al., 2005a, b; Laberg et al., 2007), are included in our inventory due to their classification as GZWs by Knies et al. (2007) and Dowdeswell et al. (2008b). The subdued relief and asymmetric wedge-shaped geometry of the landforms in Vestfjorden (e.g. Fig. 2A) are also consistent with an interpretation as GZWs.

A synthesis of the key geometric and physiographic data for each high-latitude GZW is presented in Table 2. GZW dimensions were determined from previous descriptions of each landform, together with measurements from any available bathymetric or acoustic data. In this study, GZW width was measured in an across-trough direction, perpendicular to the inferred former ice-flow direction. GZW length was measured in a trough-parallel direction. Each GZW was categorised as either a ‘surface’ or a ‘buried’ landform (Table 2). Surface or near-surface GZWs are present on or close to the sea floor and were identified on bathymetric or shallow-acoustic data (e.g. Ottesen et al., 2005a, 2008; Mosola and Anderson, 2006; Rydningen et al., 2013). Buried GZWs are present on buried horizons within the shelf stratigraphy and were identified from seismic profiles (e.g. Dowdeswell and Fugelli, 2012; Gohl et al., 2013; Batchelor et al., 2014).

4. GROUNDING-ZONE WEDGES ON HIGH-LATITUDE CONTINENTAL MARGINS

4.1 GZW locations on high-latitude margins

A total of 143 GZWs has been described from high-latitude continental shelves in the Arctic and Antarctic (Figs. 3 and 4). The GZWs are only identified within, or at the lateral margins of cross-shelf troughs or major fjord systems. These locations have been interpreted as the former sites of marine-terminating ice streams or fast-flowing outlet glaciers which, collectively, discharged ice and sediment from Quaternary ice sheets into the oceans during at least one, and often many, Quaternary glacial period (Dahlgren et al., 2002a; Dowdeswell et al., 1996; Ó Cofaigh et al., 2003; Batchelor and Dowdeswell, 2013). The association of GZWs with cross-shelf troughs and fjords reinforces the view that fast, ice-streaming flow, which provides high rates of sediment delivery to the ice margin, is necessary for GZW formation (Dowdeswell and Elverhøi, 2002; Landvik et al., 2005; Ottesen and Dowdeswell, 2009).

A buried GZW off northwest Greenland (no. 40 in Fig. 3C) provides the only exception to the association of high-latitude GZWs with cross-shelf troughs or fjords. However, it is possible that this landform, which is buried by more than 100 m of sediment, may have been produced at the margin of a former cross-shelf trough, and accompanying ice stream, which has been infilled by subsequent sedimentation (e.g. Dowdeswell et al., 2006; Sarkar et al., 2011).

Considerable variation exists in the amount of data presently available on GZWs from high-latitude continental margins (Table 2; Figs. 3 and 4). The locations and dimensions of GZWs off Norway and the western Barents Sea margin are particularly well documented (Fig. 3B) (e.g. Ottesen et al., 2005a, 2007, 2008; Winsborrow et al., 2010; Rebesco et al., 2011; Bjarnadóttir et al., 2013; Rydningen et al., 2013). By contrast, no GZWs have been reported in the small cross-shelf troughs off Baffin Island or in the Canadian Arctic Archipelago, and only one GZW has been described from a cross-shelf trough off southwest Greenland (Fig. 3C) (Ryan et al., In Press). This is probably due to the lack of high-resolution geophysical data available from these regions. Although the GZWs off northwest and northeast Greenland have been described previously in terms of their seismic architecture and dimensions (Dowdeswell and Fugelli, 2012), the map in Figure 3C reveals, for the first time, the approximate locations of these GZWs on the continental shelf.

The majority of the high-latitude GZWs recognised in Table 2 and Figures 3 and 4 are present on or close to the sea floor. The positions of these landforms therefore probably record the former locations of still-stands or minor re-advances of the Eurasian, Laurentide, Greenland and Antarctic ice sheets during the last deglaciation. A number of buried GZWs, which are interpreted to have been formed during earlier Quaternary glacial periods, have also been identified from seismic-reflection profiles in the Canadian Beaufort Sea, off Greenland and on the West Antarctic margin (Fig. 3A and C) (Dowdeswell and Fugelli, 2012; Batchelor et al., 2013a, 2014; Gohl et al., 2013). In addition, possible GZWs have been found in the Late Ordovician glacial rocks of Northern Africa (Decalf et al., In Press). The predominance of surface GZWs in our inventory suggests that many GZWs are removed by subsequent ice advances across the continental shelf, leaving reduced numbers preserved in the geological record. Indeed, it has also been observed in seismic records from high-latitude margins that the entire palaeo-shelf may be removed by particularly erosive subsequent ice advances (e.g. Dowdeswell et al., 2007). However, the relative absence of buried GZWs in our inventory could also be, in part at least, a consequence of a lack of seismic data from high-latitude margins

4.2 GZW dimensions

4.2.1 Description

Information on GZW length, in the direction of past ice flow, is provided for 84 of the Arctic and Antarctic GZWs in Table 2 and Figures 3 and 4. Although GZW lengths range between 1 and 140 km, the majority (64%) of high-latitude GZWs are less than 15 km long (Fig. 5A). Only four of the GZWs have lengths of more than 50 km (Fig. 5); a GZW in Prince Gustav Channel off the Antarctic Peninsula (no. 80 in Fig. 4A), and three GZWs in the cross-shelf troughs of the Ross Sea, West Antarctica (nos. 121, 125 and 128 in Fig. 4B). Whereas the majority (78%) of the wedges off Greenland are less than 15 km in length, only four Antarctic GZWs are less than 15 km long (Fig. 5B and C). GZW width is only available for 15 of the recorded high-latitude GZWs, and ranges between 4 and 280 km (Table 2).

The distribution of maximum sediment thickness for the 87 high-latitude GZWs for which thickness data are available is shown in Figure 6A. GZW thicknesses range between 15 and 300 m; the modal value is 60 to 80 m. Considerable variations in GZW thickness are recognised along each continental margin (Fig. 6A). However, whereas 53% of the GZWs off Greenland are more than 80 m thick (Fig. 6B), only two of the recorded Antarctic GZWs reach thicknesses of more than 80 m (Fig. 6C).

Length and maximum thickness data are available for 76 high-latitude GZWs (Fig. 7A). There is no significant correlation between GZW length and thickness when GZWs from all high-latitude margins are analysed collectively (Fig. 7A). However, when GZWs off Antarctica are removed from the inventory, GZW length is shown to have a moderate positive correlation with GZW thickness (Fig. 7B). A least-squares regression fit to these data gives a correlation coefficient, R, of 0.60, which is significant at a 99% level of probability. The scatter-plot shown in Figure 7C shows that, whereas GZWs off Greenland have a positive correlation between their length and thickness (R is 0.49, significant at 99% level of probability), there is no relationship between these variables for the GZWs identified on the Antarctic margin.

4.2.2 Interpretation

High-latitude GZWs are typically less than 15 km long and 15 to 100 m thick (Figs. 5A and 6A). This observation is in broad agreement with other studies of GZW dimensions, including Dowdeswell and Fugelli's (2012) analysis of 40 GZWs on the Greenland, Antarctic and Norwegian continental margins, which represents a sub-set of those reported here. GZWs with lengths of greater than 50 km have only been observed off Antarctica (nos. 80, 121, 125 and 128 in Fig. 4A and B). The five thickest high-latitude GZWs are located in the Canadian Beaufort Sea, off northeast Greenland and off East Antarctica (nos. 3, 4, 59, 60 and 134 in Figs. 3A, C and 4C).

When formed during a single episode of cross-shelf glaciation, large GZWs record relatively lengthy still-stands in the former ice-margin position and/or particularly high rates of sediment delivery to the grounding zone (Alley et al., 2007; Dowdeswell and Fugelli, 2012). However, many of the largest GZWs in our inventory (Table 2) are probably composite features formed during several advances of the grounding zone over successive

Quaternary glaciations (Fig. 7A and B). The GZWs at the lateral margins of the Amundsen Gulf and M'Clure Strait troughs in the Canadian Beaufort Sea (nos. 3 and 4 in Fig. 3A) have been interpreted previously as composite landforms (Batchelor et al., 2014), as have large GZWs off northwest and northeast Greenland (nos. 57 and 59 in Fig. 3C, respectively) (Dowdeswell and Fugelli, 2012). The thickest recorded GZW, the 300 m-thick GZW in Prydz Channel, East Antarctica (no. 134 in Fig. 4C), is probably also a composite feature formed over successive Quaternary glaciations (O'Brien et al., 1999).

A positive correlation between GZW length and thickness is inferred for GZWs on the Greenland, Norwegian, Canadian and Barents Sea margins (Fig. 7B). This suggests that, provided GZW development is not constrained by continental shelf topography, an increase in the volume of sediment provided to the grounding zone will result in an increase in both GZW length and thickness. GZW width, which is observed to range between 4 and 280 km (Table 2), does not scale with GZW length or thickness, and is constrained by the width of the palaeo-ice stream and any cross-shelf trough it occupies (Dowdeswell and Fugelli, 2012).

No significant relationship between GZW length and thickness exists for the GZWs described from the Antarctic margin (Fig. 7C). The data from Antarctica may be skewed by three GZWs which exhibit particularly high length-to-thickness ratios (Fig. 7C); these GZWs are located in Belgica Trough in the Bellingshausen Sea, in the Ross Sea of West Antarctica and in Mertz Trough, East Antarctica (nos. 99, 127 and 131 in Fig. 4). However, even with these three wedges removed from the dataset, the GZWs off Antarctica have higher length-to-thickness ratios than the GZWs on the Greenland margin (Fig. 7C).

The reason for the apparent difference in geometry between GZWs on the Greenland and Antarctic margins (Figs. 5, 6 and 7C) is uncertain. It is possible that the bases of thicker Antarctic ice shelves prevented the aggradation of high-amplitude wedges on this continental shelf. The higher length-to-thickness ratios of the Antarctic GZWs may reflect a more gradual seaward thinning of Antarctic ice shelves due to lower rates of basal and surface melting. The Antarctic GZWs for which length and thickness data are available all occur within cross-shelf troughs with reverse, landward-dipping slopes (Anderson, 1999; Livingston et al., 2012; Batchelor and Dowdeswell, 2013). It is possible that GZWs forming on reverse slopes may have reduced vertical accommodation space beneath an ice shelf compared with GZWs on seaward-dipping slopes. However, length and thickness data are only available for a relatively small number of Antarctic GZWs (14), compared with a larger number of GZWs reported from the Greenland margin (37).

4.3 Seismic architecture of GZWs

4.3.1 Description

High-resolution seismic data has made it possible for the internal-reflection configuration of GZWs to be resolved (e.g. Anderson, 1999; Mosola and Anderson, 2006; Dowdeswell and Fugelli, 2012). Seismic data are therefore valuable for identifying GZWs in the geological record and for distinguishing GZWs from other types of ice-marginal landforms. Surface and buried GZWs are shown to possess similar acoustic characteristics on high-latitude continental margins (Figs. 8 and 9).

GZWs are distinguished primarily by their asymmetric geometry, with steeper ice-distal sides and shallower ice-proximal sides (typically significantly less than 1°). GZW asymmetry is particularly apparent on vertically-exaggerated seismic-reflection profiles of the shelf, on which GZWs are displayed as pronounced topographic features (Figs. 8 and 9). The upper surface of a GZW is typically shown as a continuous reflection on seismic profiles. The upper GZW surface is sometimes incised by v-shaped indentations, which represent ploughmarks produced by the action of iceberg keels grounding in sea-floor sediments (Fig.

8B). The basal reflection of a GZW often truncates underlying reflections on the shelf (Fig. 8B, D). More rarely, channel-like forms, characterised by onlapping reflections and v-shaped incisions, are identified within GZWs (McMullen et al., 2006; Dowdeswell and Fugelli, 2012).

High-latitude GZWs typically possess a transparent to semi-transparent acoustic character on seismic profiles (Table 2; Figs. 8 and 9) (e.g. Ó Cofaigh et al., 2005a; Ottesen et al., 2008; Dowdeswell and Fugelli, 2012; Batchelor et al., 2014). A chaotic acoustic signature has also been described for several Antarctic GZWs (e.g. Anderson, 1999; Lowe and Anderson, 2002; Heroy and Anderson, 2005; Mosola and Anderson, 2006). High-latitude GZWs commonly contain low-angle (around 1°) reflections that dip in a seaward direction (Table 2; Figs. 8 and 9) (Larter and Vanneste, 1995; Anderson, 1999; Ó Cofaigh et al., 2005a; Dowdeswell and Fugelli, 2012; Rydningen et al., 2013; Batchelor et al., 2014).

4.3.2 Interpretation

The asymmetric geometry of high-latitude GZWs in the direction of past ice-flow (Figs. 8 and 9) reflects the conditions under which the diamictic sediment that comprises these landforms was deposited at the grounding zone and redistributed on the continental shelf. During GZW formation, the emplacement of diamictic sediment probably occurs within the low-angle roofed, water-filled cavities that exist between the sea floor and the base of ice shelves (Fig. 1A). Sediment deposition is concentrated at the ice-distal side of the GZW, allowing the wedge to build in a horizontal and seaward direction. The low-gradient ice-shelf base (Fig. 1A) restricts vertical development of the GZW, leading to the formation of a low-angle slope on the ice-proximal side of the wedge (Dowdeswell and Fugelli, 2012). Once the sediment is released at the grounding zone, it is then redistributed by gravity-flow processes to form the steeper ice-distal side of the GZW (King et al., 1991; Powell and Alley, 1997).

The truncation of underlying reflections by the basal reflection of a GZW indicates erosion prior to the time of GZW initiation (Dowdeswell and Fugelli, 2012).

The transparent to chaotic acoustic character of high-latitude GZWs (Table 2; Figs. 8 and 9) reflects the delivery of unsorted diamictic debris to the grounding zone. This sediment is probably derived predominantly from the deformable layer of sediment that has been reported to exist beneath fast-flowing ice streams (Alley et al., 1986; Blankenship et al., 1987; Canals et al., 2000; Dowdeswell et al., 2004; Ó Cofaigh et al., 2005a; Anandakrishnan et al., 2007; Smith et al., 2007; Smith and Murray, 2009; Horgan et al., 2013). The low reflectivity of GZWs may also indicate some degree of sediment reworking or deformation during short-term fluctuations in the grounding-zone position. The low-amplitude dipping reflections which have been described within many high-latitude GZWs (Table 2; Figs. 8 and 9) are interpreted to represent sediment progradation and seaward growth of the wedge through continued delivery of diamictic material supplied from the flow of active ice (Larter and Vanneste, 1995; Anderson, 1999; Ó Cofaigh et al., 2005a; Dowdeswell and Fugelli, 2012; Bjarnadóttir et al., 2013).

A number of GZWs have been shown to possess a more complex internal structure, with internal dipping reflections downlapping onto multiple erosion surfaces within the wedge (Fig. 9). Downlapping reflections within a GZW may indicate different phases of sedimentation; for example, during minor oscillations in the grounding-zone position or during different phases of wedge build-up over successive glaciations. The erosional, channel-like forms which have been identified within some high-latitude GZWs may have been produced by the flow of meltwater within subglacial channel systems (McMullen et al., 2006; Dowdeswell and Fugelli, 2012). The channel-like incisions are not topographically controlled (Dowdeswell and Fugelli, 2012), implying that meltwater flow occurred at a high water-pressure within the channels (Röthlisberger, 1972; Shreve, 1972).

GZWs on high-latitude continental margins exhibit a large degree of similarity in their morphological and acoustic characteristics (Figs. 8 and 9). This probably reflects their formation predominantly through the continued deposition of deformable till at the grounding-zone of high-latitude ice streams. GZWs appear to be largely absent from the sea floor of lower-latitude but formerly glaciated shelves, probably due to the absence of ice shelves, which are not able to survive the significant summer melting in these locations. In fact, ice shelves appear to be restricted to environments colder than the -5 °C mean annual isotherm (Vaughan and Doake, 1996). Ice-marginal depocentres on lower-latitude margins, in which ice-sheet mass loss was dominated by meltwater runoff (Siegert and Dowdeswell, 2002), were probably formed by a greater variety of processes compared with high-latitude GZWs, including a larger component of sedimentation through meltwater runoff. It is therefore possible that depocentres on lower-latitude margins, or in locations where free-flowing meltwater was abundant, exhibit a wider range of acoustic characteristics compared with GZWs on high-latitude margins. In particular, ice-marginal deposits formed in regions with abundant meltwater may contain more sorted sediments and/or erosional meltwater channels.

4.4 GZW locations on the continental shelf

Many of the high-latitude GZWs shown in Figures 3 and 4 can be categorised as one or more of four distinctive 'types' based on their location on the continental shelf: 1) at vertical pinning points in the underlying bathymetry; 2) at lateral pinning points caused by the narrowing of a cross-shelf trough or fjord; 3) on the outermost shelf; and 4) at the outer-shelf lateral margins of a cross-shelf trough (Table 2 and Fig. 10). This classification is based on information on GZWs provided in previous studies, together with observations of available bathymetric and acoustic data. A location 'type' is lacking for a number of the GZWs described in Table 2. In these cases, there may be a lack of information available about the GZW and the geometry of the surrounding shelf. Alternatively, the location at which the GZW formed may have been interpreted to have been largely uninfluenced by the geometry of the shelf.

4.4.1 Vertical pinning points

Description

A number of high-latitude GZWs occur in association with bathymetric highs that have been interpreted to have provided vertical pinning points for ice stabilisation during retreat (Table 2; Figs. 8F, 10A and B) (Echelmeyer et al., 1991; Joughin et al., 2004; Ottesen et al., 2007; Dowdeswell and Fugelli, 2012). Examples of GZWs formed at vertical pinning points include several of the wedges off northwest Greenland (nos. 39, 42 and 46 in Fig. 3C) and the two most landward GZWs in eastern Pine Island Trough, West Antarctica, which are also associated with lateral constrictions of the trough (nos. 106 and 107 in Fig. 4A). The GZW shown in Figure 8F, which was identified using newly-available seismic reflection data from the northwest Greenland margin, is interpreted to have formed at this location due to a prominent bedrock high in the underlying bathymetry.

Interpretation

Although the position of still-stands during retreat of an ice margin is dependent on a number of factors, including ice-sheet mass balance, the geometry of the continental shelf can influence the locations at which GZWs form through exerting a fundamental control on grounding-zone stability (Dowdeswell and Siegert, 1999; Venteris, 1999; Schoof, 2007; Nick et al., 2009; Gudmundsson et al., 2012; Jamieson et al., 2012). Shallower water depths caused by topographic highs encourage stabilisation of the grounding zone through reducing the mass flow across the grounding zone, assuming a constant ice velocity. Bedrock outcrops on the sea floor can act as vertical pinning points (e.g. Fig. 8F), as can accumulations of sediment that were deposited during earlier still-stands of the grounding zone (e.g. Rüther et al., 2011).

The retreat style of an ice stream can be influenced greatly by the gradient and slope-direction of a cross-shelf trough or fjord. The grounding zones of ice streams which extend across seaward-dipping regions of the shelf have been suggested to be inherently more stable than for ice streams on reverse, landward-dipping slopes in which the sea-floor becomes progressively deeper inshore (e.g. Schoof, 2007; Nick et al., 2009; Katz and Worster, 2010). Ice streams which retreat through cross-shelf troughs with seaward-dipping slopes may therefore be more likely to undergo episodic patterns of ice retreat, in which retreat is punctuated by grounding-zone still-stands and GZW development, compared with ice streams that retreat through troughs with reverse gradient slopes, which may be more susceptible to rapid ice retreat (Dowdeswell et al., 2008; Graham et al., 2010; Livingstone et al., 2012).

Geophysical observations and modelling experiments indicate that periods of relative stability in ice retreat may coincide with low-gradient areas, or benches, in sea-floor topography (Weertman, 1974; Schoof, 2007; Graham et al., 2010). For example, the five GZWs in eastern Pine Island Trough, West Antarctica (nos. 103 to 107 in Fig. 4A) have been interpreted to have formed in association with low-gradient benches in the trough's long-profile (Graham et al., 2010). Conversely, regions of the trough that have steeper reverse-bed slopes lack evidence for grounding-zone stabilisation, suggesting phases of rapid ice retreat (Dowdeswell et al., 2008; Graham et al., 2010).

Although the depth and gradient of the sea floor can influence the position of still-stands in a retreating ice margin, rapid ice retreat does not necessarily occur on reverse slopes or at vertical pinning points (Shipp et al., 2002; Dowdeswell et al., 2008; Ó Cofaigh et al., 2008). GZWs are present on reverse, landward-dipping slopes in a large number of cross-shelf troughs, including Marguerite, Belgica, Pine Island and Getz–Dotson troughs off Antarctica (nos. 87 to 112 in Fig. 4A), where they indicate periods of stabilisation in the former grounding zone (Lowe and Anderson, 2002; Ó Cofaigh et al., 2005a, b; Graham et al., 2009, 2010; Jamieson et al., 2012; Kirshner et al., 2012).

4.4.2 Lateral pinning points

Description

A number of high-latitude GZWs occur in association with a reduction in the across-trough width of a cross-shelf trough or fjord (Table 2; Fig. 10C and D). These locations have been suggested to act as lateral pinning points for grounding-zone stabilisation during retreat (Ottesen et al., 2005a; Jamieson et al., 2012). GZWs have been interpreted previously to have formed at lateral pinning points on the western Svalbard and Norwegian margins (nos. 12, 13 and 28 to 31 in Fig. 3B) (Ottesen et al., 2005a, 2007, 2008; Winsborrow et al., 2010), in Arctic Canada (no. 2 in Fig. 3A) (Batchelor et al., 2014), and in Marguerite Trough, Antarctic Peninsula (nos. 87 to 98 in Fig. 4A) (Jamieson et al., 2012).

Interpretation

A reduction in the width of a cross-shelf trough or fjord encourages grounding-zone stability through increasing the lateral drag that is exerted on the glacier and its floating ice shelf (Echelmeyer et al., 1991, 1994; Whillans and van der Veen, 1997; Joughin et al., 2004).

The increase in lateral drag restricts the flow rate across the grounding zone. Ice-sheet thickening and surface steepening will occur upstream of the lateral pinning point in order to balance the increased lateral drag with an increase in the force that drives ice flow. In a recent numerical simulation of ice-stream retreat through Marguerite Trough on the Antarctic Peninsula, Jamieson et al. (2012) suggested that the locations of eight GZWs within the trough (nos. 87 to 94 in Fig. 4A) corresponded with lateral pinning points at the trough sides. Although the ice stream width was parameterised and the trough margins were estimated from sparse regional bathymetry data in the flow-band model of Jamieson et al. (2012), their study demonstrates the influence of trough width as a control on grounding-zone stability.

Reductions in cross-shelf trough width are often caused by the position of shallow banks or islands on the continental shelf, which act as lateral pinning points for ice stabilisation during retreat (e.g. Fig. 10C and D). Still-stands in the ice-margin position commonly occur at fjord mouths (e.g. nos. 14 and 28 in Table 2 and Fig. 3B), where the ice stream becomes constrained by fjord and valley-wall morphology. Still-stands in the ice-margin position can also occur as a result of the narrowing of cross-shelf troughs on the middle-shelf (e.g. nos. 54 and 55 in Fig. 3C). The majority of cross-shelf troughs in the High Arctic widen significantly towards the shelf break as a result of ice emerging from the constraints of fjords or inter-island channels into open-shelf settings in which topographic control was lost (Batchelor and Dowdeswell, 2014). Many High Arctic ice streams therefore experienced a reduction in width as they retreated back inland from the wider outer-shelf to the more constrained geometry of the middle- and inner-shelf.

4.4.3 Outermost continental shelf

<u>Description</u>

Some high-latitude GZWs occur on the outermost continental shelf of cross-shelf troughs (Fig. 10E and F). GZWs are identified close to the shelf break on the western Svalbard and Norwegian margins (nos. 18, 32 and 34 in Fig. 3B), on the northwest and northeast Greenland margins (nos. 45, 61, 64 and 67 in Fig. 3C) and off West Antarctica (nos. 116, 124 and 126 in Fig. 4B). A seismic example of a GZW formed on the outermost shelf within Melville Bay Trough, northwest Greenland is shown in Figure 8E. The landform close to the shelf break in Melville Bay Trough (Fig. 8E) is interpreted as a GZW due to its asymmetric geometry and low-amplitude internal reflections which dip in a seaward direction. The continental slope beyond Melville Bay Trough has also been interpreted as the site of a major trough-mouth fan (Ó Cofaigh et al., 2013; Batchelor and Dowdeswell, 2014). The GZW which is identified on the outermost shelf of the trough (Fig. 8E) is distinct from the trough-mouth fan on the adjacent slope. Whereas GZWs have positive-relief geometry and are formed mainly through subglacial deposition of deforming till at the grounding zone during still-stands in an ice-margin position, trough-mouth fans are composed predominantly of glacigenic-debris flows which are produced by the rapid delivery of deformable sediment to the shelf break and subsequent down-slope sediment transfer during full-glacial periods (Dowdeswell et al., 1998; Elverhøi et al., 1998; Vorren et al., 1998; Dowdeswell and Siegert, 1999).

<u>Interpretation</u>

The rapid delivery of deformable sediment to the shelf edge by fast-flowing ice streams typically results in the formation of trough-mouth fans on the continental slope (Fig. 1C) (Vorren et al., 1998; Dowdeswell and Siegert, 1999). However, the occasional presence of GZWs on the outermost continental shelf in cross-shelf troughs (Fig. 10E and F) implies that the ice-stream grounding zone stabilised in this position, probably for a period of at least several decades. Further advance of the grounding zone into deepening water on the upper continental slope is unlikely and there is little morphological evidence of streamlined landforms beyond the shelf breaks of many high-latitude margins. Accumulations of sediment that were deposited during previous still-stands of the ice margin can sometimes act as vertical pinning points close to the shelf break (Rüther et al., 2011).

4.4.4 Outer-shelf lateral margins

Description

Several high-latitude GZWs are located at the outer-shelf lateral margins of cross-shelf troughs (Figs. 9, 10G and H). GZWs have been described from the outer-shelf lateral margins of the Amundsen Gulf and M'Clure Strait troughs in the Canadian Beaufort Sea (nos. 3 and 4 in Fig. 3A) (Batchelor et al., 2014), an unnamed trough and Uummannaq Trough off northwest Greenland (nos. 53 and 57 in Fig. 3C), and off the Antarctic Peninsula (nos. 83 and 84 in Fig. 4A) (Larter and Vanneste, 1995; Vanneste and Larter, 1995). Some of these GZWs are shown to possess a complex internal structure, with internal dipping reflections downlapping onto multiple erosion surfaces within the wedge (Fig. 9).

Interpretation

The GZWs which have been identified from the outer-shelf lateral margins of high-latitude cross-shelf troughs possess similar dimensions and acoustic character to other high-latitude GZWs (Figs. 8 and 9). However, the locations of these wedges imply that they are not classical GZWs formed at the terminus of an ice stream (Dowdeswell and Fugelli, 2012). These landforms are, instead, interpreted as lateral GZWs which developed through the delivery of till to the outer-shelf lateral margins of an ice stream (Batchelor et al., 2014).

With lengths of 15 to 50 km and maximum thicknesses of 60 to 200 m, the six lateral GZWs (Table 2) are too large to be shear-zone moraines (e.g. Dyke and Morris, 1988; Stokes and Clark, 2002).

The lateral GZWs may represent the boundary between fast, ice-streaming flow in the troughs and slower, cold-based ice on the adjacent shelf. However, if the wedges were formed at the margin between fast- and slow-flowing ice, the net sediment transfer direction would probably be predominantly from the region of slow-flowing ice and higher elevation towards the region of fast ice flow within the deeper troughs. In contrast, the dipping internal reflections within the lateral GZWs demonstrate that sediment was transported predominantly from the troughs towards the adjacent shallow shelf (Fig. 9).

It is possible that the lateral GZWs formed at the boundary between ice in the troughs and an ice-free zone on the shelf, or where streaming ice flow diverged as it entered an ice shelf. Development of lateral GZWs was probably encouraged by the geometry of the continental shelf, with the shallower inter-trough regions of the shelf leading to reduced rates of iceberg calving and a still-stand in the grounding zone. It is also possible that the lateral GZWs are the remnants of wider GZWs which were formed close to the shelf break. The section of the GZWs which was formed directly in front of the cross-shelf troughs may have been eroded and removed by one or more subsequent ice-stream advances, leaving only the lateral parts of each landform preserved on the sea floor.

The lateral GZWs are probably composite features which were formed as ice streams repeatedly expanded their outer-shelf lateral margins (Laberg et al., 2007; Dowdeswell and Fugelli, 2012). The downlapping reflections and multiple erosion surfaces that have been identified within the lateral GZWs (Fig. 9) indicate different phases of wedge build-up over successive glaciations. The pinching out of younger sequences against the ice-proximal sides of the lateral GZWs (Fig. 9A and C) provides further evidence for multiple phases of sediment delivery to the wedges.

5. DISCUSSION

5.1 GZWs in the geological record

The inventory of GZWs presented in Table 2 and Figures 3 and 4 provides a synthesis of the locations and morphological characteristics of GZWs on high-latitude continental margins. A number of these GZWs have been categorised previously as till deltas or till tongues, or have been subsumed under the classification of moraines (e.g. Larter and Vanneste, 1995; Ottesen et al., 2005a; Laberg et al., 2007). We propose that high-latitude GZWs exhibit a variety of distinguishing characteristics that generally enable them to be differentiated from other types of ice-marginal landforms, including moraine ridges (Fig. 2), in the geological record.

High-latitude GZWs are typically less than 15 km long and 15 to 100 m thick (Figs. 5 to 7). GZWs are formed along a line-source at the grounding zone; their lateral width is therefore constrained by the width of the palaeo-ice stream, which can reach several hundreds of kilometres (Table 2). High-latitude GZWs are asymmetric in the direction of former ice-flow with steeper ice-distal sides (Figs. 8 to 10). They possess relatively high length-to-height ratios compared with higher-amplitude moraine ridges (Powell, 1984; Ottesen and Dowdeswell, 2006). GZWs possess a transparent to chaotic acoustic character (Table 2; Figs. 8 and 9), which reflects the delivery of unsorted diamictic debris to the grounding zone. The majority of high-latitude GZWs are characterised by low-amplitude dipping internal reflections (Table 2; Figs. 8 and 9), which are interpreted to represent sediment progradation and seaward growth of the GZW through continued delivery of diamictic material supplied from the flow of active ice (Larter and Vanneste, 1995; Anderson, 1999; Ó Cofaigh et al., 2005a; Dowdeswell and Fugelli, 2012).

In contrast, terminal and recessional moraines (Fig. 2) generally possess smaller dimensions than GZWs; moraines are typically less than 2 km long in the former ice-flow direction (Sexton et al., 1992; Seramur et al., 1997; Ottesen and Dowdeswell, 2006, 2009; Ottesen et al., 2007). Moraines have a clear positive relief and lower length-to-height ratios compared with the more subdued GZWs (Fig. 2A and B). Although they are composed of unsorted ice-contact sediments, and therefore possess a chaotic to transparent acoustic character (Stoker and Holmes, 1991; Sexton et al., 1992; King, 1993; Shaw, 2003), moraines generally lack the prograding internal reflections that are diagnostic of GZWs.

Although high-latitude GZWs exhibit a large degree of similarity in their morphological and acoustic characteristics (Table 2; Figs. 8 and 9), it may not be possible to categorise all ice-marginal landforms as either GZWs, moraines or ice-proximal fans (Fig. 2). Some landforms have been interpreted to exhibit characteristics of more than one ice-proximal landform; for example, the wedges in Kveithola Trough on the western Barents Sea margin (nos. 18 to 22 in Fig. 3B) possess the dimensions, asymmetric geometry and homogeneous sediments of GZWs, yet also have ice-proximal fans on their distal slopes (Bjarnadóttir et al., 2013). GZWs which formed in regions with relatively greater meltwater inputs may contain a larger component of sorted sediments, erosional meltwater channels or ice-proximal fans than those in settings where mass loss across the grounding zone was dominated by iceberg calving (Dowdeswell and Fugelli, 2012; Bjarnadóttir et al., 2013).

5.2 GZWs and palaeo-ice sheet reconstruction

The identification of GZWs in the geological record can provide important insights into the form and flow of palaeo-ice sheets.

5.2.1 Ice-streams

GZWs have been interpreted previously as part of a typical ice-stream landform assemblage (Fig. 1C); their presence, in association with deformation till, MSGL or lateral moraines, can be used to infer the former location of an ice stream on the continental shelf (Dowdeswell et al., 2008; Ottesen and Dowdeswell, 2009). In addition, the asymmetric geometry of GZWs, which have steeper ice-distal sides and shallower ice-proximal sides (Figs. 8 to 10), enables the former direction of ice-stream flow to be established.

In this study, the strong association between high-latitude GZWs and cross-shelf troughs or fjords (Figs. 3 and 4) reinforces the suggestion that fast, ice-streaming flow, which provides high rates of sediment delivery to the ice margin, is necessary for GZW formation (Dowdeswell and Elverhøi, 2002; Landvik et al., 2005; Ottesen and Dowdeswell, 2009). We therefore propose that GZWs are indicators of palaeo-ice stream activity.

5.2.2 Ice-margin still-stands and their duration

GZWs indicate periods of grounding-zone stabilisation; they can therefore provide information about the location and duration of still-stands or re-advances in the ice margin during retreat (e.g. Shipp et al., 1999; Mosola and Anderson, 2006; Ottesen et al., 2007; Dowdeswell et al., 2008). GZWs are formed predominantly through the rapid delivery of deforming subglacial sediments to the grounding zone (King et al., 1991; Powell and Alley, 1997). Fluxes of around 100 m^3 per year per metre of ice-stream width have been estimated for the delivery of diamictic subglacial sediment to an actively-forming GZW at the grounding zone of the modern Whillans Ice Stream, West Antarctica (Engelhardt and Kamb, 1997; Anandakrishnan et al., 2007). A sediment flux of between 100 and 800 m^3 per year per metre of ice-stream width has been estimated for the palaeo-ice stream draining Marguerite Trough, Antarctic Peninsula (Dowdeswell et al., 2004).

If sediment flux across the grounding zone is known, GZW volume can be used to estimate the duration of a still-stand in the ice margin (Howat and Domack, 2003). GZWs of the dimensions shown in Table 2 and Figures 5 to 7, which are typically tens of metres thick and several tens of kilometres long, are probably produced during ice-margin still-stands of at least several decades to centuries, which allow for depocentres with volumes of between ten and several hundred cubic kilometres to build up at a relatively stable grounding zone (Larter and Vanneste, 1995; Alley et al., 2007; Anandakrishnan et al., 2007; Dowdeswell et al., 2008; Dowdeswell and Fugelli, 2012).

Calculations of the duration of GZW formation are greatly dependent on the thickness of the deforming sediment layer beneath the ice stream. The thickness of this deforming sediment layer has been estimated to be a few tens of cm thick for the Whillans Ice Stream in West Antarctica (Anandakrishnan et al., 2007), whereas Dowdeswell et al.'s (2004) calculation for Marguerite Trough, Antarctic Peninsula assumed a 1 m-thick deforming sediment layer.

5.2.3 Ice shelves

It is difficult to discern the former extent and thickness of ice shelves during Quaternary full-glacial periods. Sea-floor lineations on bathymetric highs, including the Chukchi Borderlands and Lomosonov Ridge in the Arctic Ocean, may provide evidence of occasional grounding of ice-keels from ice shelves which developed during several Quaternary glaciations (Polyak et al., 2001; Jakobsson et al., 2005; Niessen et al., 2013). Sub-ice shelf sediments can also be identified occasionally from the sedimentological record (Powell, 1984; Domack et al., 1999; Kilfeather et al., 2011). Facies successions related to ice-shelf retreat typically include a distal, ice-shelf glacimarine or open-marine facies, which comprises bioturbated muds and ice-rafted debris, overlying a diamicton, gravel-rich and sand-rich ice-shelf glacimarine facies that was deposited through sub-ice shelf sediment rain-out, bottom current activity and sediment gravity flows, overlying a subglacial facies consisting predominantly of basal till deposited beneath grounded ice (Evans and Pudsey, 2002). However, there is much complexity in glacimarine lithofacies and it can be difficult to differentiate between open glacimarine and sub-ice shelf sediments in the sedimentological record.

GZWs are likely to be diagnostic of the former presence of ice shelves. The low-gradient ice-roofed cavities of ice shelves probably force the development of GZWs through restricting vertical accommodation space and preventing the build-up of high-amplitude ridges (Powell, 1990; Dowdeswell and Fugelli, 2012). However, the presence of a GZW in the geological record does not permit any inferences about the offshore extent of the former ice shelf beyond the grounding zone. The absence of GZWs from the terrestrial record, in which arcuate moraine ridges typically build up at the margins of fast-flowing ice streams (e.g. Evans et al., 2008), also supports the view that floating ice shelves are required for GZW formation.

5.3 Controls on GZW formation

GZW formation is ultimately the consequence of the delivery of sediment to the grounding zone during a still-stand in the ice-margin in the presence of an ice shelf that restricts vertical accommodation. The formation of GZWs requires high-rates of sediment delivery to a marine margin that is relatively stable for at least decades to centuries (Fig. 11).

5.3.1 Glaciological controls

GZW formation can be associated with periods of ice-sheet thickening or gradual thinning. Still-stands in the grounding-zone position, leading to sediment progradation, are caused by factors that reduce ablation or increase accumulation on the ice sheet. External, climatically-forced thickening of an ice sheet can be triggered by a decrease in ocean or atmospheric temperature, a fall in sea level, or an increase in snowfall (Fig. 11). The stability of the ice-margin is also influenced by internal ice-sheet dynamics, including the rate of inland-ice delivery to the grounding-zone and the degree of coupling between the grounding zone and the upstream ice-sheet basin (Jamieson et al., 2012). GZWs are also formed when the rate of sediment delivery to the grounding zone exceeds the rate at which space is produced at the upper surface of a GZW by ice thinning, leading to sediment aggradation.

The stability of the grounding zone may be influenced by ice-stream/ice shelf/ sediment interactions. It has been suggested that the present stability of the Whillans Ice Stream, West Antarctica is caused by a several km-long zone of reduced basal lubrication near the grounding zone (Christianson et al., 2013; Horgan et al., 2013). The zone of reduced basal lubrication is interpreted to have been formed by the compaction of subglacial till as a result of the downward flexing of grounded ice from the rising or falling tide (Christianson et al., 2013; Horgan et al., 2013).

5.3.2 Shelf topography

Although the stability of an ice margin is determined by external climatic factors and internal ice-sheet dynamics, the precise location of any still-stand or re-advance in the grounding-zone position is influenced strongly by the geometry of the continental shelf (Fig. 11). Vertical and lateral pinning points within cross-shelf troughs and fjords (Fig. 10) encourage grounding-zone stability through increasing the basal and lateral drag that is exerted on the ice stream and its floating ice shelf, and by reducing the mass flow across the grounding zone (e.g. Echelmeyer et al., 1991; Hughes, 1992; Dowdeswell and Siegert, 1999; Joughin et al., 2004; Schoof, 2007; Gudmundsson et al., 2012).

Vertical pinning points (Figs. 8F, 10A and B) can be produced by bedrock or sedimentary topographic highs that reduce the depth of the sea floor. The preferential formation of GZWs at topographic highs in cross-shelf troughs or fjords may lead to the repeated occupation of the same grounding-zone position and the formation of composite GZWs. Lateral GZWs, which have been observed at the outer-shelf lateral margins of several high-latitude cross-shelf troughs (Figs. 9, 10G and H), are interpreted to have been formed at the boundary between ice in the troughs and an ice-free zone on the shelf, or where streaming ice flow diverged as it entered an ice shelf (Batchelor et al., 2014). Lateral pinning points (Fig. 10C and D) are caused by a narrowing in the width of a cross-shelf trough or fjord. Lateral pinning points typically occur at fjord mouths, at locations where shallow banks or islands cause a reduction in trough width, and at middle-shelf locations where an ice stream may experience a reduction in width compared with its unconstrained position on the wider outer-shelf.

5.3.3 GZW formation as a mechanism for grounding-zone stability

The process of GZW formation, in which sediment aggradation occurs within water-filled cavities below ice shelves (Figs. 1A and 11), may provide a mechanism for ice-sheet stabilisation through filling any space that is produced immediately below the ice-shelf base at the grounding zone by ice thinning (Alley et al., 2007; Anandakrishnan et al., 2007). In addition, when a GZW is present, the increased frictional drag produced by greater ice-sediment contact has been suggested to slow and thicken the ice above the GZW crest. The ice thickness at the grounding zone can become greater than that needed to allow floatation.

GZW growth may therefore counteract grounding-zone retreat induced by small (< 10 m) relative sea-level rise, possibly preventing or postponing rapid ice-sheet collapse (Alley et al., 2007; Anandakrishnan et al., 2007). Although GZWs may provide a mechanism for grounding-zone stabilisation, this feedback is dependent upon the initial formation of a GZW, which is controlled ultimately by variations in the rate of sediment delivery, the rate of ice thinning, and the pre-existing geometry of the continental shelf.

6. CONCLUSIONS

Ice-proximal landforms, including GZWs, moraine ridges and ice-proximal fans (Fig. 2), build up at the grounding zone of marine-terminating ice sheets during still-stands or re-advances of the ice margin. The identification of ice-proximal landforms in the geological record can provide information about former ice-sheet dynamics and the locations of any still-stands or re-advances in the grounding-zone position (e.g. Shipp et al., 1999; Mosola and Anderson, 2006; Ottesen et al., 2007; Dowdeswell et al., 2008; Benn and Evans, 2010). GZWs are asymmetric wedges of sediment that are formed through the rapid delivery of sediment to the grounding zone (Powell and Domack, 1995; Powell and Alley, 1997). A number of GZWs have been described previously from high-latitude continental shelves in both hemispheres (e.g. Ó Cofaigh et al., 2005a; Evans et al., 2006; Mosola and Anderson, 2006; Ottesen et al., 2007, 2008; Rydningen et al., 2013), where they have been interpreted to indicate episodic palaeo-ice-stream retreat punctuated by still-stands in the grounding-zone position (Dowdeswell et al., 2008; Ó Cofaigh et al., 2008).

We have presented an inventory of 143 high-latitude GZWs (Table 2; Figs. 3 and 4) which is compiled from available bathymetric and acoustic data, in addition to newly-available 2-D seismic reflection data from the northwest and northeast Greenland margins. A synthesis of the key morphological and acoustic characteristics of GZWs, which enable them to be differentiated from other types of ice-proximal landforms on high-latitude continental shelves, such as moraine ridges and ice-proximal fans (Fig. 2), is provided.

Sea floor and buried GZWs possess similar acoustic and morphological characteristics on all high-latitude margins on which they have been identified (Table 2; Figs. 8 to 10). GZWs are asymmetric in the direction of former ice-flow with steeper ice-distal sides (Figs. 8 to 10), and have relatively high length-to-height ratios compared with high-amplitude moraine ridges (Fig. 2) (Powell, 1984; Ottesen and Dowdeswell, 2006). They possess a transparent to chaotic character on acoustic profiles (Table 2; Figs. 8 and 9), which reflects the delivery of unsorted diamictic debris to the grounding zone. The majority of high-latitude GZWs contain low-amplitude dipping reflections (Table 2; Figs. 8 and 9), which are interpreted to represent seaward growth of the wedge through continued delivery of diamictic material to the grounding zone (Larter and Vanneste, 1995; Anderson, 1999; Ó Cofaigh et al., 2005a; Dowdeswell and Fugelli, 2012).

The identification and description of GZWs in the geological record provides valuable information about the form and flow of palaeo-ice sheets. The strong association between high-latitude GZWs and cross-shelf troughs or fjords (Figs. 3 and 4) suggests that GZW formation requires relatively high rates of sediment delivery to the grounding zone by fast-flowing ice streams or outlet glaciers. The asymmetric geometry of GZWs (Figs. 8 to 10) also enables the direction of former ice-streaming flow to be interpreted. GZWs are formed preferentially by ice sheets with termini ending as floating ice shelves (Fig. 11) (King and Fader, 1986; King et al., 1987; Powell and Alley, 1997). The low-gradient ice-roofed cavities of ice shelves (Fig. 1A) force GZW formation through restricting vertical accommodation space and preventing the build-up of high-amplitude moraine ridges (Powell, 1990; Dowdeswell and Fugelli, 2012).

GZWs indicate the locations of significant (at least decades to centuries) still-stands in the grounding-zone position (Larter and Vanneste, 1995; Alley et al., 2007; Anandakrishnan et al., 2007; Dowdeswell et al., 2008; Livingstone et al., 2012). The precise location at which the grounding zone halts or re-advances is often controlled strongly by the geometry of the continental shelf (Fig. 11). Many high-latitude GZWs occur at vertical and lateral pinning points within cross-shelf troughs or fjords (Fig. 10A to D), which encourage grounding-zone stability through increasing the basal and lateral drag that is exerted on the ice stream and reducing the mass flow across the grounding zone (Echelmeyer et al., 1991; Hughes, 1992; Dowdeswell and Siegert, 1999; Joughin et al., 2004; Schoof, 2007; Dowdeswell and Fugelli, 2012; Gudmundsson et al., 2012).

7. ACKNOWLEDGEMENTS

We thank TGS-NOPEC Geophysical Company ASA for permission to reproduce 2-D seismic reflection data from the northwest and northeast Greenland margins, and Phil O'Brien, Dag Ottesen and Michele Rebesco for the use of acoustic and bathymetric data modified for this work. We thank Rob Larter and one anonymous reviewer for their helpful comments.

8. REFERENCES

Alley, R.B., Blankenship, D.D., Bentley, C.R., Rooney, S.T., 1986. Deformation of till beneath Ice Stream B, West Antarctica. *Nature 322*, 57–59.

Alley, R.B., Blankenship, D.D., Bentley, C.R., Rooney, S.T., 1987. Till beneath ice stream B. 3. Till deformation: evidence and implications. *Journal of Geophysical Research 92*, 8921-8929.

Alley, R.B., Blankenship, D.D., Rooney, S.T., Bentley, C.R., 1989. Sedimentation beneath ice shelves - the view from ice stream B. *Marine Geology 85*, 101-120.

Alley, R.B., Anandakrishnan, S., Dupont, T.K., Parizek, B.R., Pollard, D., 2007. Effect of sedimentation on ice-sheet grounding-line stability. *Science 315*, 1838-1841.

Anandakrishnan, S., Catania, G.A., Alley, R.B., Horgan, H.J., 2007. Discovery of till deposition at the grounding line of Whillans Ice Stream. *Science 315*, 1835-1838.

Anderson, J.B., Bartek, L.R., 1992. Ross Sea glacial history revealed by high resolution seismic reflection data combined with drill site information. *In:* Kennett, J.P., Warnke, D.E. (Eds.), *The Antarctic Paleoenvironment: A Perspective on Global Change 1*. Antarctic Research Series. American Geophysical Union, Washington, DC, 56, 231-263.

Anderson, J.B., Shipp, S.S., Bartek, L.R., Reid, D.E., 1992. Evidence for a grounded ice sheet on the Ross Sea continental shelf during the late Pleistocene and preliminary paleodrainage reconstruction. *In:* Elliot, D.H. (Ed.), *Contributions to Antarctica Research III*. Antarctic Research Series. American Geophysical Union, Washington, DC, *57*, 39–62.

Anderson, J.B., 1997. Grounding zone wedges on the Antarctic continental shelf, Weddell Sea. *In:* Davies, T.A., Bell, T., Cooper, A.K., Josenhans, H., Polyak, L., Solheim, A., Stoker,

M. S., Stravers, J.A. (Eds.), *Glaciated Continental Margins: An Atlas of Acoustic Images*, 968–970. Chapman & Hall, London.

Anderson, J.B., 1999. *Antarctic Marine Geology*. Cambridge University Press.

Anderson, J.B., Shipp, S.S., Lowe, A.L., Wellner, J.S., Mosola, A.B., 2002. The Antarctic Ice Sheet during the Last Glacial Maximum and its subsequent retreat history: a review. *Quaternary Science Reviews 21*, 49-70.

Andreassen, K., Laberg, J.S., Vorren, T.O., 2008. Seafloor geomorphology of the SW Barents Sea and its glaci-dynamic implications. *Geomorphology 97*, 157-177.

Andreassen, K., Winsborrow, M.C.M., Bjarnadóttir, L.R., Rüther, D.C., 2014. Ice stream retreat dynamics inferred from an assemblage of landforms in the northern Barents Sea. *Quaternary Science Reviews 92*, 246-257.

Bart, P.J., Anderson, J.B., 1991. Grounding zone wedges of the Antarctic continental shelf, Antarctic Peninsula. *In:* Davies, T.A., Bell, T., Cooper, A.K., Josenhans, H., Polyak, L., Solheim, A., Stoker, M.S., Stravers, J.A. (Eds.), *Glaciated continental margins: an atlas of acoustic images*. Chapman and Hall, London.

Bart, P.J., 2004. West-directed flow of the West Antarctic Ice Sheet across eastern basin, Ross Sea during the Quaternary. *Earth and Planetary Science Letters 228*, 425-438.

Bart, P., Owolana, B., 2012. On the duration of West Antarctic Ice Sheet grounding events in the Ross Sea during the Quaternary. *Quaternary Science Reviews 47*, 101-115.

Batchelor, C.L., Dowdeswell, J.A., 2014. The physiography of High Arctic cross-shelf troughs. *Quaternary Science Reviews 92*, 68-96.

Batchelor, C.L., Dowdeswell, J.A., Pietras, J.T., 2013a. Variable history of Quaternary ice-sheet advance across the Beaufort Sea margin, Arctic Ocean. *Geology 41*, 131-134.

Batchelor, C.L., Dowdeswell, J.A., Pietras, J.T., 2013b. Seismic stratigraphy, sedimentary architecture and palaeo-glaciology of the Mackenzie Trough: evidence for two Quaternary ice advances and limited fan development on the western Canadian Beaufort Sea margin. *Quaternary Science Reviews 65*, 73-87.

Batchelor, C.L., Dowdeswell, J.A., Pietras, J.T., 2014. Evidence for multiple Quaternary ice advances and fan development from the Amundsen Gulf cross-shelf trough and slope, Canadian Beaufort Sea margin. *Marine and Petroleum Geology 52*, 125-143.

Benn, D., Evans, D.J.A., 2010. *Glaciers and glaciation*. 2nd Edition. Hodder Arnold Publication.

Bennett, M.R., Boulton, G.S., 1993. A reinterpretation of Scottish 'hummocky moraine' and its significance for the deglaciation of the Scottish Highlands during the Younger Dryas or Loch Lomond Stadial. *Geological Magazine 130*, 301-318.

Bentley, M.J., Anderson, J.B., 1998. Glacial and marine geological evidence for the ice sheet configuration in the Weddell Sea - Antarctic Peninsula region during the Last Glacial Maximum. *Antarctic Science 10*, 309–325.

Bindschadler, R.A., King, M.A., Alley, R.B., Anandakrishnan, S., Padman, L., 2003. Tidally controlled stick-slip of a West Antarctic ice stream. *Science 301*, 1087–1089.

Bjarnadóttir, L.R., Rüther, D.C., Winsborrow, M.C.M., Andreassen, K., 2013. Grounding-line dynamics during the last deglaciation of Kveithola, W Barents Sea, as revealed by seabed geomorphology and shallow seismic stratigraphy. *Boreas 42*, 84-107.

Blankenship, D.D., Bentley, C.R., Rooney, S.T., Alley, R.B., 1987. Till beneath ice stream B 1. Properties derived from seismic travel times. *Journal of Geophysical Research 92*, 8903-8911.

Bond, G., Heinrich, H., Broecker, W., Labeyrie, L., McManus, J., Andrews, J., Huon, S., Jantschik, R., Clasen, S., Simet, C., Tedesco, K., Klas, M., Bonani, G., Ivy, S., 1992. Evidence for massive discharges of icebergs into the glacial northern Atlantic. *Nature 360*, 245-250.

Boulton, G.S., 1986. Push-moraines and glacier-contact fans in marine and terrestrial environments. *Sedimentology 33*, 677-698.

Boulton, G.S., Van der Meer, J.J.M., Hart, J., Beets, D., Ruegg, G.H.J., Van der Wateren, F.M., Jarvis, J., 1996. Till and moraine emplacement in a deforming bed surge - an example from a marine environment. *Quaternary Science Reviews 15*, 961–987.

Bradwell, T., Stoker, M.S., Golledge, N.R., Wilson, C., Merrit, J., Long, D., Everest, J.D., Hestvik, O.B., Stevenson, A., Hubbard, A., Finlayson, A., Mathers, H., 2008. The northern sector of the Last British Ice Sheet: maximum extent and demise. *Earth Science Reviews 88*, 207-226.

Brown, C.S., Meier, M.F., Post, A., 1982. *Calving speed of Alaska tidewater glaciers, with application to Columbia Glacier*. U.S. Geological Survey Professional Paper 1258-C.

Cai, J., Powell, R.D., Cowan, E.A., Carlson, P.R., 1997. Lithofacies and seismic-reflection interpretation of temperate glacimarine sedimentation in Tarr Inlet, Glacier Bay, Alaska. *Marine Geology 143*, 5-37.

Canals, M., Urgeles, R., Calafat, A.M., 2000. Deep sea-floor evidence of past ice streams off the Antarctic Peninsula. *Geology 28*, 31-34.

Christ, A.J., Talaia-Murray, M., Elking, N., Domack, E.W., Leventer, A., Lavoie, C., Brachfeld, S., Yoo, K-C., Gilbert, R., Jeong, S-M., Petrushak, S., Wellner, J., 2014. Late Holocene glacial advance and ice shelf growth in Barilari Bay, Graham Land, west Antarctic Peninsula. *Geological Society of America Bulletin 127*, 297-315.

Christianson, K., Parizek, B.R., Alley, R.B., Horgan, H.J., Jacobel, R.W., Anandakrishnan, S., Keisling, B.A., Craig, B.D., Muto, A., 2013. Ice sheet grounding zone stabilisation due to till compaction. *Geophysical Research Letters 40*, 5406-5411.

Christoffersen, P., Tulaczyk, S., Behar, A., 2010. Basal ice sequences in Antarctic ice stream: exposure of past hydrologic conditions and a principal mode of sediment transfer. *Journal of Geophysical Research 115*, F03034.

Clark, C.D., Hughes, A.L.C., Greenwood, S.L., Jordan, C., Sejrup, H.P., 2012. Pattern and timing of retreat of the last British-Irish Ice Sheet. *Quaternary Science Reviews 44*, 112-146.

Dahlgren, K.I.T., Vorren, T.O., Laberg, J.S., 2002a. The role of grounding-line sediment supply in ice-sheet advances and growth on continental shelves: an example from the mid Norwegian sector of the Fennoscandian ice sheet during the Saalian and Weichselian. *Quaternary International 95-96*, 25-33.

Dahlgren, K.I.T., Vorren T.O., Laberg, J.S., 2002b. Late Quaternary glacial development of the mid-Norwegian margin – 65 to 68° N. *Marine and Petroleum Geology 19*, 1089-1113.

Decalf, C., Dowdeswell, J.A., Fugelli, E.M.G., In Press. Seismic character of possible buried grounding-zone wedges in the Late Ordovician glacial rocks of Algeria. *In:* Dowdeswell, J.A., Canals, M., Jakobsson, M., Todd, B.T., Dowdeswell, E.K., Hogan, K.A. (Eds.), *Atlas of submarine glacial landforms: modern, Quaternary and ancient.* Geological Society, London, Memoirs.

Domack, E.W., O'Brien, P., Harris, P., Taylor, F., Quilty, P., DeSantis, L., Raker, B., 1998. Late Quaternary sediment facies in Prydz Bay, east Antarctica and their relationship to glacial advance onto the continental shelf. *Antarctic Science 10*, 236-246.

Domack, E.W., Jacobson, E.A., Shipp, S., Anderson, J.B., 1999. Late Pleistocene-Holocene retreat of the West Antarctic Ice-Sheet system in the Ross Sea: Part 2 – Sedimentological and stratigraphic signature. *Geological Society of America Bulletin 111*, 1517-1536.

Dowdeswell, J.A., Elverhøi, A., 2002. The timing of initiation of fast-flowing ice streams during a glacial cycle inferred from glacimarine sedimentation. *Marine Geology 188*, 3-14.

Dowdeswell, J.A., Fugelli, E.M.G., 2012. The seismic architecture and geometry of grounding-zone wedges formed at the marine margins of past ice sheets. *Geological Society of America Bulletin 124*, 1750-1761.

Dowdeswell, J.A., Siegert, M.J., 1999. Ice-sheet numerical modelling and marine geophysical measurements of glacier-derived sedimentation on the Eurasian Arctic continental margins. *Geological Society of America Bulletin 111*, 1080-1097.

Dowdeswell, J.A., Vasquez, M., 2013. Submarine landforms in the fjords of southern Chile: implications for glacimarine processes and sedimentation in a mild glacier-influenced environment. *Quaternary Science Reviews 64*, 1-19.

Dowdeswell, J.A., Villinger, H., Whittington, R.J., Marienfeld, P., 1993. Iceberg scouring in Scoresby Sund and on the East Greenland continental shelf. *Marine Geology 111*, 37-53.

Dowdeswell, J.A., Uenzelmann-Neben, G., Whittington, R.J., Marienfeld, P., 1994. The Late Quaternary sedimentary record in Scoresby Sund, East Greenland. *Boreas 23*, 294-310.

Dowdeswell, J.A., Kenyon, N., Elverhøi, A., Laberg, J.S., Mienert, J., Siegert, M.J., 1996. Large-scale sedimentation on the glacier influenced Polar North Atlantic margins: long-range side-scan sonar evidence. *Geophysical Research Letters 23*, 3535–3538.

Dowdeswell, J.A., Elverhøi, A., Spielhagen, R., 1998. Glacimarine sedimentary processes and facies on the Polar North Atlantic margins. *Quaternary Science Reviews 17*, 243-272.

Dowdeswell, J.A., Ó Cofaigh, C., Pudsey, C.J., 2004. Thickness and extent of the subglacial till layer beneath an Antarctic paleo-ice stream. *Geology 32*, 13-16.

Dowdeswell, J.A., Ottesen, D., Rise, L., 2006. Flow-switching and large-scale deposition by ice streams draining former ice sheets. *Geology 34*, 313-316.

Dowdeswell, J.A., Ottesen, D., Rise, L., Craig, J., 2007. Identification and preservation of landforms diagnostic of past ice-sheet activity on continental shelves from three-dimensional seismic evidence. *Geology 35*, 359-362.

Dowdeswell, J.A., Ottesen, D., Evans, J., Ó Cofaigh, C., Anderson, J.B., 2008. Submarine glacial landforms and rates of ice-stream collapse. *Geology 36*, 819–822.

Dowdeswell, J.A., Hogan, K.A., Ó Cofaigh, C., Fugelli, E.M.G., Evans, J., Noormets, R., 2014. Late Quaternary ice flow in a West Greenland fjord and cross-shelf trough system: submarine landforms from Rink Isbrae to Uummannaq shelf and slope. *Quaternary Science Reviews 92*, 292-309.

Dowdeswell, J.A., Hogan, K.A., Arnold, N.S., Mugford, R.I., Wells, M., Hirst, J.P.P., Decalf, C., In Press. Sediment-rich meltwater plumes and ice-proximal fans at the margins of modern and ancient tidewater glaciers: observations and modelling. *Sedimentology*.

Dreimanis, A., Hamilton, J.P., Kelly, P.E., 1987. Complex subglacial sedimentation of Catfish Creek till at Bradtville, Ontario, Canada. *In:* Van der Meer, J.J.M. (Ed.), *Tills and glaciotectonics*. Rotterdam, Balkema, 73-87.

Dunlop, P., Shannon, R., McCabe, M., Quinn, R., Doyle, E., 2010. Marine geophysical evidence for ice sheet extension and recession on the Malin Shelf: New evidence for the western limits of the British Irish Ice Sheet. *Marine Geology 276*, 86-99.

Dyke, A.S., Morris, T.F., 1988. Drumlin fields, dispersal trains and ice streams in Arctic Canada. *Canadian Geographic 32*, 86-90.

Dyke, A.S., Andrews, J.T., Clark, P.U., England, J.H., Miller, G.H., Shaw, J., Veillette, J.J., 2002. The Laurentide and Innuitian ice sheets during the Last Glacial Maximum. *Quaternary Science Reviews 21*, 9–31.

Echelmeyer, K., Clarke, T.S., Harrison, W.D., 1991. Surficial glaciology of Jakobshavn Isbræ, West Greenland: Part 1. Surface morphology. *Journal of Glaciology 37*, 368-382.

Echelmeyer, K.A., Harrison, W.D., Larsen, C., Mitchell, J.E., 1994. The role of the margins in the dynamics of an active ice stream. *Journal of Glaciology 40*, 527-538.

Ehlers, J., Gibbard, P.L., 2007. The extent and chronology of Cenozoic global glaciation. *Quaternary International 164-165*, 6-20.

Elvenes, S., Dowdeswell, J.A., In Press. Possible 'lift-off moraines' at grounded ice-sheet margins, North Norwegian shelf edge. *In:* Dowdeswell, J.A., Canals, M., Jakobsson, M., Todd, B.T., Dowdeswell, E.K., Hogan, K.A. (Eds.), *Atlas of submarine glacial landforms: modern, Quaternary and ancient.* Geological Society, London, Memoirs.

Elverhøi, A., Lønne, Ø., Seland, R., 1983. Glaciomarine sedimentation in a modern fjord environment, Spitsbergen. *Polar Research 1*, 127-149.

Elverhøi, A., Hooke, R., Le, B., Solheim, A., 1998. Late Cenozoic erosion and sediment yield from the Svalbard-Barents Sea region: implications for understanding erosion of glacierised basins. *Quaternary Science Reviews 17*, 209-242.

Enderlin, E.M., Howat, I.M., 2013. Submarine melt rate estimates for floating termini of Greenland outlet glaciers. *Journal of Glaciology 59*, 67-75.

Evans, J., Pudsey, C.J., 2002. Sedimentation associated with Antarctic Peninsula ice shelves: Implications for palaeoenvironmental reconstructions of glacimarine sediments. *Journal of the Geological Society London 159*, 233-237.

Evans, J., Pudsey, C.J., Ó Cofaigh, C., Morris, P.W., Domack, E.W., 2005. Late Quaternary glacial history, dynamics and sedimentation of the eastern margin of the Antarctic Peninsula Ice Sheet. *Quaternary Science Reviews 24*, 741-774.

Evans, J., Dowdeswell, J.A, Ó Cofaigh, C., Benham, T.J., Anderson, J.B., 2006. Extent and dynamics of the West Antarctic Ice Sheet on the outer continental shelf of Pine Island Bay during the last glaciation. *Marine Geology 230*, 53-72.

Evans, D.J.A., Clark, C.D., Rea, B.R., 2008. Landform and sediment imprints of fast glacier flow in the southwest Laurentide Ice Sheet. *Journal of Quaternary Science 23*, 249-272.

Forwick, M., Vorren, T.O., 2011. Stratigraphy and deglaciation of the Isfjorden area, Spitsbergen. *Norwegian Journal of Geology 90*, 163–179.

Gilbert, R., Domack, E.W., Camerlenghi, A., 2003. Deglacial history of the Greenpeace Trough: ice sheet to ice shelf transition in the northern Weddell Sea. *In:* Domack, E., Leventer, A., Burnett, A., Bindschadler, R., Peter, C., Kirby, M. (Eds.), *Antarctic Peninsula Climate Variability; Historical and Paleoenvironmental Perspectives.* Antarctic Research Series 79, 195–204.

Gohl, K., Uenzelmann-Neben, G., Larter, R.D., Hillenbrand, C-D., Hochmuth, K., Kalberg, T., Weigelt, E., Davy, B., Kuhn, G., Nitsche, F.O., 2013. Seismic stratigraphic record of the Amundsen Sea Embayment shelf from pre-glacial to recent times: evidence for a dynamic West Antarctic ice sheet. *Marine Geology 344*, 115-131.

Graham, A.G.C., Larter, R.D., Gohl, K., Hillenbrand, C.-D., Smith, J.A., Kuhn, G., 2009. Bedform signature of a West Antarctic palaeo-ice stream reveals a multitemporal record of flow and substrate control. *Quaternary Science Reviews 28*, 2774-2793.

Graham, A.G.C., Larter, R.D., Gohl, K., Dowdeswell, J.A., Hillenbrand, C.-D., Smith, J.A., Evans, J., Kuhn, G., Deen, T., 2010. Flow and retreat of the late Quaternary Pine Island-Thwaites palaeo-ice stream, West Antarctica. *Journal of Geophysical Research 115*, F03025.

Greenwood, S.L., Gyllencreutz, R., Jakobsson, M., Anderson, J.B., 2012. Ice-flow switching and East/West Antarctic Ice Sheet roles in glaciation of the western Ross Sea. *Geological Society of American Bulletin 124*, 1736-1749.

Gudmundsson, G.H., 2007. Tides and the flow of Rutford ice stream, West Antarctica. *Journal of Geophysical Research 112*, F04007.

Gudmundsson, G.H., Krug, J., Durand, G., Favier, L., Gagliardini, O., 2012. The stability of grounding lines on retrograde slopes. *The Cryosphere Discussions 6*, 2597-2619.

Hagen, J.O., 1987. Glacier surge at Usherbreen, Svalbard. *Polar Research 5*, 239–252.

Hanebuth, T.J.J., Rebesco, M., Urgeles, R., Lucchi, R., Freudenthal, T., 2014. Drilling glacial deposits in offshore polar regions. *Eos, Transactions American Geophysical Union 95*, 277-278.

Heroy, D.C., Anderson, J.B., 2005. Ice-sheet extent of the Antarctic Peninsula region during the Last Glacial Maximum (LGM) - insights from glacial geomorphology. *Geological Society of America Bulletin 117*, 1497-1512.

Hirst, J.P.P., 2012. Ordovician proglacial sediments in Algeria: insights into the controls on hydrocarbon reservoirs in the In Amenas Field, Illizi Basin. *In:* Husse, M., Redfern, J., Le Heron, D., Dixon, R.J., Moscariello, A., Craig, J. (Eds.), *Glaciogenic Reservoirs and Hydrocarbon Systems*. Geological Society, London, Special Publications 368, 319-353.

Hodgson, D.A., Graham, A.G.C., Griffiths, H.J., Roberts, S.J., Ó Cofaigh, C., Bentley, M.J., Evans, D.J.A., 2014. Glacial history of sub-Antarctic South Georgia based on the submarine geomorphology of its fjords. *Quaternary Science Reviews 89*, 129-147.

Hogan, K.A., Dowdeswell, J.A., Noormets, R., Evans, J., Ó Cofaigh, C., Jakobsson, M., 2010. Submarine landforms and ice-sheet flow in the Kvitøya Trough, northwestern Barents Sea. *Quaternary Science Reviews 29*, 3545–3562.

Holtedahl, H., 1989. Submarine end moraines and associated deposits off the south coast of Norway. *Marine Geology 88*, 23-48.

Horgan, H.J., Christianson, K., Jacobel, R.W., Anandakrishnan, S., Alley, R.B., 2013. Sediment deposition at the modern grounding zone of Whillans Ice Stream, West Antarctica. *Geophysical Research Letters 40*, 3934-3939.

Howat, I.M., Domack, E.W., 2003. Reconstructions of western Ross Sea palaeo-ice stream grounding zones from high-resolution acoustic stratigraphy. *Boreas 32*, 56-75.

Hughes, T., 1992. Theoretical calving rates from glaciers along ice walls grounded in water of variable depths. *Journal of Glaciology 38*, 282-294.

Hunter, L.E., Powell, R.D., Smith, G.W., 1996. Facies architecture and grounding-line fan processes of morainal banks during the deglaciation of Coastal Maine. *Geological Society of America Bulletin 108*, 1022-1038.

Jakobsson, M., Gardner, J.V., Vogt, P., Mayer, L.A., Armstrong, A., Backman, J., Brennan, R., Calder, B., Hall, J.K., Kraft, B., 2005. Multibeam bathymetric and sediment profiler evidence for ice grounding on the Chukchi Borderland, Arctic Ocean. *Quaternary Research 63*, 150-160.

Jakobsson, M., Anderson, J.B., Nitsche, F.O., Gyllencreutz, R., Kirshner, A., Kirchner, N., O'Regan, M.A., Mohammad, R., Eriksson, B., 2012a. Ice sheet retreat dynamics inferred from glacial morphology of the central Pine Island Bay Trough, West Antarctica. *Quaternary Science Reviews 38*, 1-10.

Jakobsson, M., Mayer, L., Coakley, B., Dowdeswell, J.A., Forbes, S., Fridman, B., Hodnesdal, H., Noormets, R., Pedersen, R., Rebesco, M., Schenke, H.W., Zarayskaya, Y., Accettella, D., Armstrong, A., Anderson, R.M., Bienhoff, P., Camerlenghi, A., Church, I., Edwards, M., Gardner, J.V., Hall, J.K., Hell, B., Hestvik, O., Kristoffersen, Y., Marcussen, C., Mohammad, R., Mosher, D., Nghiem, S.V., Pedrosa, M.T., Travaglini, P.G., Weatherall, P., 2012b. The International Bathymetric Chart of the Arctic Ocean (IBCAO) Version 3.0. *Geophysical Research Letters 39*, L12609.

Jamieson, S.S.R., Vieli, A., Livingstone, S.J., Ó Cofaigh, C., Stokes, C., Hillenbrand, C-D., Dowdeswell, J.A., 2012. Ice-stream stability on a reverse bed slope. Nature Geoscience 5, 799-802.

Jenkins, A., Doake, C.S.M., 1991. Ice-ocean interaction on Ronne Ice Shelf, Antarctica. *Journal of Geophysical Research 96*, 791–813.

Joughin, I., Abdalati, W., Fahnestock, M., 2004. Large fluctuations in speed on Greenland's Jakobshavn Isbrae glacier. *Nature 432*, 608-610.

Katz, R.F., Worster, M.G., 2010. Stability of ice-sheet grounding lines. *Proceedings of the Royal Society A – Mathematical, Physical and Engineering Sciences 466*, 1597-1620.

Kilfeather, A.A., Ó Cofaigh, C., Lloyd, J.M., Dowdeswell, J.A., Xu, S., Moreton, S.G., 2011. Ice-stream retreat and ice-shelf history in Marguerite Trough, Antarctic Peninsula: sedimentological and foraminiferal signatures. *Geological Society of America Bulletin 123*, 997-1015.

King, L.H., Fader, G.B., 1986. Wisconsinan glaciation of the continental shelf – Southeast Atlantic Canada. *Geological Survey of Canada Bulletin 363*.

King, L.H., Rokoengen, K., Gunleiksrud, T., 1987. Quaternary seismostratigraphy of the Mid Norwegian Shelf, 65°-67°30'N – a till tongue stratigraphy. *Continental Shelf Institution (IKU), Publication 114*, 58pp.

King, L.H., Rokoengen, K., Fader, G.B.J., Gunleiksrud, T., 1991. Till-tongue stratigraphy. *Geological Society of America Bulletin 103*, 637-659.

King, E.L., 1993. Till in the marine environment. *Journal of Quaternary Science 8*, 347-358.

Kirshner, A.E., Anderson, J.B., Jakobsson, M., O'Regan, M., Majewski, W., Nitsche, F.O., 2012. Post-LGM deglaciation in Pine Island Bay, West Antarctica. *Quaternary Science Reviews 38*, 11-26.

Klages, J.P., Kuhn, G., Hillenbrand, C.-D., Graham, A.G.C., Smith, J.A., Larter, R.D., Gohl, K., 2013. First geomorphological record and glacial history of an inter-ice stream ridge on the West Antarctic continental shelf. *Quaternary Science Reviews 61*, 47-61.

Klages, J.P., Kuhn, G., Hillenbrand, C.-D., Graham, A.G.C., Smith, J.A., Larter, R.D., Gohl, K., Wacker, L., 2014. Retreat of the West Antarctic Ice Sheet from the western Amundsen Sea shelf at a pre- or early LGM stage. *Quaternary Science Reviews 91*, 1-15.

Knies, J., Vogt, C., Matthiessen, J., Nam, S.-I., Ottesen, D., Rise, L., Bargel, T., Eilertsen, R.S., 2007. Re-advance of the Fennoscandian Ice Sheet during Heinrich Event 1. *Marine Geology 240*, 1-18.

Laberg, J.S, Vorren, T.O., Dowdeswell, J.A., Kenyon, N.H., Taylor, J., 2000. The Andøya Slide and the Andøya Canyon, north-eastern Norwegian-Greenland Sea. *Marine Geology 162*, 259-275.

Laberg, J.S., Eilertsen, R.S., Salomonsen, G.R., Vorren, T.O., 2007. Submarine push moraine formation during the early Fennoscandian Ice Sheet deglaciation. *Quaternary Research 67*, 453–462.

Laberg, J.S., Eilertsen, R., Vorren, T.O., 2009. The paleo–ice stream in Vestfjorden, north Norway, over the last 35 k.y.: Glacial erosion and sediment yield. *Geological Society of America Bulletin 121*, 434–447.

Laberg, J.S., Forwick, M., Husum, K., 2014. The NE Greenland Ice Sheet during the last glacial – a dynamic retreat from the shelf edge triggered by ice melting? *Geophysical Research Abstracts 16*, EGU2014-2075.

Landvik, J., Ingólfsson, Ó., Mienert, J., Lehman, S., Solheim, A., Elverhøi, A., Ottesen, D., 2005. Rethinking Late Weichselian ice sheet dynamics in coastal NW Svalbard. *Boreas 34*, 7-24.

Larter, R.D., Barker, P.F., 1989. Seismic stratigraphy of the Antarctic Peninsula Pacific margin: A record of Pliocene-Pleistocene ice volume and paleoclimate. *Geology 17*, 731-734.

Larter, R.D., Vanneste, L.E., 1995. Relict subglacial deltas on the Antarctic Peninsula outer shelf. *Geology 23*, 33-36.

Larter, R.D., Graham, A.G.C., Hillenbrand, C-D., Smith, J.A., Gales, J.A., 2012. Late Quaternary grounded ice extent in the Filchner Trough, Weddell Sea, Antarctica: new marine geophysical evidence. *Quaternary Science Reviews 53*, 111-122.

Li, G., Piper, D.J., Calvin Campbell, D., 2011. The Quaternary Lancaster Sound trough-mouth fan, NW Baffin Bay. *Journal of Quaternary Science 26*, 511–522.

Liestøl, O., 1976. Årsmorener foran Nathorstbreen? *Norsk Polarinstitutt Årbok 1976*, 361–363.

Lindén, M., Möller, P., 2005. Marginal formation of De Geer moraines and their implications to the dynamics of grounding-line recession. *Journal of Quaternary Science 20*, 113-133.

Livingstone, S.J., Ó Cofaigh, C., Stokes, C.R., Hillenbrand, C.-D., Vieli, A., Jamieson, S.S.R., 2012. Antarctic palaeo-ice streams. *Earth-science Reviews 111*, 90-128.

Livingstone, S.J., Ó Cofaigh, C., Stokes, C.R., Hillenbrand, C.-D, Vieli, A., Jamieson, S.S.R., 2013. Glacial geomorphology of Marguerite Bay Palaeo-Ice stream, western Antarctic Peninsula. *Journal of Maps 9*, 558-572.

Lønne, I., 1993. Physical signatures of ice-advance in a Younger Dryas ice-contact delta, Troms, northern Norway: Implications for glacier-terminus history. *Boreas 22*, 59-70.

Lønne, I., 1995. Sedimentary facies and depositional architecture of ice-contact glaciomarine systems. *Sedimentary Geology 98*, 13-43.

Lønne, I., 1997. Sedimentology and depositional history of an early Holocene ice-contact submarine fan: The Egge-Lyngås 'end-moraine', southern Norway. *Norske Geologisk Tidsskrift 77*, 137-157.

Lønne, I., Nemec, W., Blikra, L.H., Lauritsen, T., 2001. Sedimentary architecture and dynamic stratigraphy of the marine ice-contact system. *Journal of Sedimentary Research 71*, 922-943.

Lucchi, R.G., Pedrosa, M.T., Camerlenghi, A., Urgeles, R., De Mol, B., Rebesco, M., 2012. Recent submarine landslides on the continental slope of Storfjorden and Kveithola Trough-Mouth Fans (northwest Barents Sea). *In:* Yamada, Y., Kawamura, K., Ikehara, K., Ogawa, Y., Urgeles, R., Mosher, D., Chaytor, J., Strasser, M. (Eds.), *Submarine Mass Movements and Their Consequences, Advances in Natural and Technological Hazards Research 31.* Springer, Dordrecht, pp. 735-745.

Mackintosh, A., Golledge, N., Domack, E., Dunbar, R., Leventer, A., White, D., Pollard, D., DeConto, R., Fink, D., Zwartz, D., Gore, D., Lavoie, C., 2011. Retreat of the East Antarctic ice sheet during the last glacial termination. *Nature Geoscience 4*, 195-202.

McMullen, K., Domack, E., Leventer, A., Olson, C., Dunbar, R., Brachfeld, S., 2006. Glacial morphology and sediment formation in the Mertz Trough, East Antarctic. *Paleogeography, Palaeoclimatology, Palaeoecology 231*, 169-180.

Mosola, A.B., Anderson, J.B., 2006. Expansion and rapid retreat of the West Antarctic Ice Sheet in eastern Ross Sea: Possible consequence of over-extended ice streams? *Quaternary Science Reviews 25*, 2177–2196.

Mugford, R., Dowdeswell, J.A., 2011. Modeling glacial meltwater plume dynamics and sedimentation in high-latitude fjords. *Journal of Geophysical Research 116*, F01023.

Murray, T., Smith, A.M., King, M.A., Weedon, G.P., 2007. Ice flow modulated by tides at up to annual periods at Rutford ice stream, West Antarctica. *Geophysical Research Letters 34*, L18503.

Nick, F.M., Vieli, A., Howat, I.M., Joughin, I., 2009. Large-scale changes in Greenland outlet glacier dynamics triggered at the terminus. *Nature Geoscience 2*, 110-114.

Niessen, F., Hong, J.K., Hegewald, A., Matthiessen, J., Stein, R., Kim, H., Kim, S., Jensen, L., Jokat, W., Nam, S.-I., Kang, S.-H., 2013. Repeated Pleistocene glaciation of the East Siberian Continental Margin. *Nature Geoscience 6*, 842-846.

Noormets, R., Hogan, K., Austin, W., Chauhan, T., Roy, S., Rasmussen, T., Dowdeswell, J., 2012. Submarine glacial landform assemblages on the outer continental shelf north of

Nordaustlandet, Svalbard. *The 6th Arctic Paleoclimate and its Extremes (APEX) Meeting, Program and Abstracts,* Oulu University, 15-18 May. Oululanka Research Station, Finland, p. 70.

Nygård, A., Sejrup, H.P., Haflidason, H., Cecci, M., Ottesen, D., 2004. The deglaciation history of the southwestern Fennoscandian Ice Sheet between 15 and 13 14C ka. *Boreas 33*, 1-17.

Nygård, A., Sejrup, H.P., Haflidason, H., Bryn, P., 2005. The glacial North Sea Fan, southern Norwegian Margin: architecture and evolution from the upper continental slope to the deep-sea basin. *Marine and Petroleum Geology 22*, 71-84.

Ó Cofaigh, C., Pudsey, C.J., Dowdeswell, J.A., Morris, P., 2002. Evolution of subglacial bedforms along a paleo-ice stream, Antarctic Peninsula continental shelf. *Geophysical Research Letters 29*, 41-1 – 41-4.

Ó Cofaigh, C., Taylor, J., Dowdeswell, J.A., Pudsey, C.J., 2003. Palaeo-ice streams, trough mouth fans and high-latitude continental slope sedimentation. *Boreas 32*, 37–55.

Ó Cofaigh, C., Dowdeswell, J.A., Allen, C.S., Hiemstra, J., Pudsey, C.J., Evans, J., Evans, D.J.A., 2005a. Flow dynamics and till genesis associated with a marine-based Antarctic palaeo-ice stream. *Quaternary Science Reviews 24*, 709–740.

Ó Cofaigh, C., Larter, R.D., Dowdeswell, J.A., Hillenbrand, C.-D., Pudsey, C.J., Evans, J., Morris, P., 2005b. Flow of the West Antarctic Ice Sheet on the continental margin of the

Bellingshausen Sea at the Last Glacial Maximum. *Journal of Geophysical Research 110*, B11103.

Ó Cofaigh, C., Dowdeswell, J.A., Evans, J, Larter, R.D., 2008. Geological constraints on Antarctic palaeo-ice-stream retreat. *Earth Surface Processes and Landforms 33,* 513-525.

Ó Cofaigh, C., Dunlop, P., Benetti, S., 2012. Marine geophysical evidence for Late Pleistocene ice sheet extent and recession off northwest Ireland. *Quaternary Science Reviews 44*, 147-159.

Ó Cofaigh, C., Andrews, J.T., Jennings, A.E., Dowdeswell, J.A., Hogan, K.A., Kilfeather, A.A., Sheldon, C., 2013. Glacimarine lithofacies, provenance and depositional processes on a West Greenland trough-mouth fan. *Journal of Quaternary Science 28,* 13-26.

O'Brien, P.E., Goodwin, I., Forsberg, C.-F., Cooper, A.K., Whitehead, J., 2007. Late Neogene ice drainage changes in Prydz Bay, East Antarctica and the interaction of Antarctic ice sheet evolution and climate. *Palaeogeography, Palaeoclimatology, Palaeoecology 245*, 390-410.

Ottesen, D., Dowdeswell, J.A., 2006. Assemblages of submarine landforms produced by tidewater glaciers in Svalbard. *Journal of Geophysical Research 111*, F01016.

Ottesen, D., Dowdeswell, J.A., 2009. An inter-ice stream glaciated margin: submarine landforms and a geomorphic model based on marine-geophysical data from Svalbard. *Geological Society of America, Bulletin 121*, 1647–1665.

Ottesen, D., Dowdeswell, J.A., Rise, L., Rokoengen, K., Henriksen, S., 2002. Large-scale morphological evidence for past ice-stream flow on the mid-Norwegian continental margin. *In:* Dowdeswell, J.A., Ó Cofaigh, C. (Eds.), *Glacier-influenced Sedimentation in High-latitude Continental Margins*, Geological Society, London, Special Publication, vol. 203, pp. 245-258.

Ottesen, D., Dowdeswell, J.A., Rise, L., 2005a. Submarine landforms and the reconstruction of fast-flowing ice streams within a large Quaternary ice sheet: the 2500-km-long Norwegian-Svalbard margin (57° to 80°N). *Geological Society of America Bulletin 117*, 1033-1050.

Ottesen, D., Rise, L., Knies, J., Olsen, L., Henriksen, S., 2005b. The Vestfjorden-Trænadjupet paleo-ice stream drainage system, mid-Norwegian continental shelf. *Marine Geology 218*, 175-189.

Ottesen, D., Dowdeswell, J.A., Lanvik, J.Y., Mienert, J., 2007. Dynamics of the Late Weichselian ice sheet on Svalbard inferred from high-resolution sea-floor morphology. *Boreas 36*, 286-306.

Ottesen, D., Stokes, C.R., Rise, L., Olsen, L., 2008. Ice-sheet dynamics and ice streaming along the coastal parts of northern Norway. *Quaternary Science Reviews 27*, 922-940.

Overpeck, J.T., Peterson, L.C., Kipp, N., Imbrie, J., Rind, D., 1989. Climate change in the circum-North Atlantic region during the last deglaciation. *Nature 338*, 553–557.

Pedrosa, M.T., Camerlenghi, A., De Mol, B., Urgeles, R., Rebesco, M., Lucchi, R.G., 2011. Seabed morphology and shallow sedimentary structure of the Storfjorden and Kveithola trough-mouth fans (northwest Barents Sea). *Marine Geology 286*, 65-81.

Polyak, L., Edwards, M.H., Coakley, B.J., Jakobsson, M., 2001. Ice shelves in the Pleistocene Arctic Ocean inferred from glaciogenic deep-sea bedforms. *Nature 410*, 453-459.

Powell, R.D., 1981. A model for sedimentation by tidewater glaciers. *Annals of Glaciology 2*, 129-134.

Powell, R.D., 1983. Glacial-marine sedimentation processes and lithofacies of temperate tidewater glaciers, Glacier Bay, Alaska. *In:* Molnia, B.F. (Ed.), *Glacial-Marine Sedimentation*, 185-232. Plenum Press, New York.

Powell, R.D., 1984. Glacimarine processes and inductive lithofacies modelling of ice shelf and tidewater glacier sediment based on Quaternary examples. *Marine Geology 57*, 1-52.

Powell, R.D., 1990. Processes at glacial grounding-line fans and their growth to ice-contact deltas. *In:* Dowdeswell, J.A., Scourse, J.D. (Eds.), *Glacimarine Environments: Processes and Sediments*. Geological Society of London Special Publication 53, 53-73.

Powell, R.D., 1991. Grounding-line systems as second order controls on fluctuations of temperate tidewater termini. *In:* Ashley, G.M., Anderson, J.B. (Eds.), *Glacial Marine*

Sedimentation - Paleoclimatic Significance. Geological Society of American Special Paper 261, 75-94.

Powell, R.D., Alley, R.B., 1997. Grounding-line systems: processes, glaciological inferences and the stratigraphic record. *In:* Barker, P.F., Cooper, A.C. (Eds.), *Geology and seismic stratigraphy of the Antarctic Margin II.* Antarctic Research Series. American Geophysical Union, Washington, DC, 71, 169-187.

Powell, R.D., Domack, E.W., 1995. Modern glaciomarine environments. *In:* Menzies, J. (Ed.), *Glacial Environments: Volume 1. Modern Glacial Environments: Processes, Dynamics and Sediments.* Butterworth-Heinmann, Oxford, 445-486.

Powell, R., Domack, E., 2002. Modern glaciomarine environments. *In:* Menzies, J. (Ed.), *Modern and Past Glacial Environments,* 361-389. Butterworth-Heinemann, Boston.

Powell, R.D., Dawber, M., McInnes, J.N., Pyne, A.R., 1996. Observations of the grounding line area at a floating glacier terminus. *Annals of Glaciology 22,* 217-223.

Pritchard, H.D., Arthern, R.J., Vaughan, D.G., Edwards, L.A., 2009. Extensive dynamic thinning on the margins of the Greenland and Antarctic ice sheets. *Nature 461,* 971–975.

Rebesco, M., Lui, Y., Camerlenghi, A., Winsborrow, M., Laberg, J.S., Caburlotto, A., Diviacco, P., Accettella, D., Sauli, C., Wardell, N., Tomini, I., 2011. Deglaciation of the western margin of the Barents Sea Ice Sheet – A swath bathymetric and sub-bottom seismic study from the Kveithola Trough. *Marine Geology 279,* 141-147.

Rebesco, M., Domack, E., Zgur, F., Lavoie, C., Leventer, A., Brachfeld, S., Willmott, V., Halberson, G., Truffer, M., Scambos, T., Smith, J., Pettit, E., 2014. Boundary condition of grounding lines prior to collapse, Larsen-B Ice Shelf, Antarctica. *Science 345*, 1354-1358.

Retelle, M.J., Bither, K.M., 1989. Late Wisconsinan glacial and glaciomarine sedimentary facies in the lower Androscoggin Valley, Topsham, Maine. *In:* Tucker, R.D., Marvinney, R.G. (Eds.), *Studies in Marine geology, Volume 6: Quaternary geology.* Augusta, Maine, Maine Geological Survey, 33-51.

Rignot, E., Jacobs, S.S., 2002. Rapid bottom melting widespread near Antarctic ice sheet grounding lines. *Science 296*, 2020-2023.

Rignot, E., Kanagaratnam, P., 2006. Changes in the velocity structure of the Greenland Ice Sheet. *Science 311*, 986-989.

Rignot, E., Bamber, J.L., van den Broeke, M.R., Davis, C., Li, Y., van de Berg, W.J., van Meijgaard, E., 2008. Recent Antarctic ice mass loss from radar interferometry and regional climate modelling. *Nature Geoscience 1*, 106-110.

Rise, L., Ottesen, D., Berg, K., Lundin, E., 2002. Large-scale development of the mid-Norwegian margin during the last 3 million years. *Marine and Petroleum Geology 22*, 33-44.

Röthlisberger, H., 1972. Water pressure in intra- and subglacial channels. *Journal of Glaciology 11*, 177-203.

Rüther, D.C., Mattingsdal, R., Andreassen, K., Forwick, M., Husum, K., 2011. Seismic architecture and sedimentology of a major grounding zone system deposited by the Bjørnøyrenna Ice Stream during Late Weichselian deglaciation. *Quaternary Science Reviews 30*, 2776-2792.

Ryan, J.C., Dowdeswell, J.A., Hogan, K.A., In Press. Three cross-shelf troughs on the continental shelf of Southwest Greenland from Olex data. *In:* Dowdeswell, J.A., Canals, M., Jakobsson, M., Todd, B.T., Dowdeswell, E.K., Hogan, K.A. (Eds.), *Atlas of submarine glacial landforms: modern, Quaternary and ancient.* Geological Society, London, Memoirs.

Rydningen, T.A., Vorren, T.O., Laberg, J.S., Kolstad, V., 2013. The marine-based NW Fennoscandian ice sheet: glacial and deglacial dynamics as reconstructed from submarine landforms. *Quaternary Science Reviews 68*, 126-141.

Sarkar, S., Berndt, C., Chabert, A., Masson, D.G., Minshull, T.A., Westbrook, G.K., 2011. Switching of a paleo-ice stream in northwest Svalbard. *Quaternary Science Reviews 30*, 1710–1725.

Schoof, C., 2007. Ice sheet grounding line dynamics: steady states, stability, and hysteresis. *Journal of Geophysical Research 112*, F03S28.

Seramur, K.C., Powell, R.D., Carlson, P.R., 1997. Evaluation of conditions along the grounding line of temperate marine glaciers: an example from Muir Inlet, Glacier Bay, Alaska. *Marine Geology 140*, 307-327.

Sexton, D.J., Dowdeswell, J.A., Solheim, A., Elverhøi, A., 1992. Seismic architecture and sedimentation in north-west Spitsbergen fjords. *Marine Geology 103*, 53-68.

Sharp, M., 1985. 'Crevasse-fill' ridges – a landform type characteristic of surging glacier? *Geografiska Annaler 67*, 213-220.

Shaw, J., Todd, B.J., Brushett, D., Parrott, D.R., Bell, T., 2009. Late Wisconsinan glacial landsystems on Atlantic Canadian shelves: new evidence from multibeam and single-beam sonar data. *Boreas 38*, 146–159.

Shaw, J., 2003. Submarine moraines in Newfoundland coastal waters: implications for the deglaciation of Newfoundland and adjacent areas. *Quaternary International 99-100*, 115–134.

Shepherd, A., Wingham, D., 2007. Recent sea-level contributions of the Antarctic and Greenland ice sheets. *Science 315*, 1529–1532.

Shipp, S., Anderson, J.B., 1997. Grounding zone wedges on the Antarctic continental shelf, Ross Sea. *In:* Davies, T.A., Josenhans, H., Polyak, L., Solheim, A., Stoker, M.S., Stravers, J.A. (Eds.), *Glaciated Continental Margins, an Atlas of Acoustic Images*. Chapman & Hall, London, 104–105.

Shipp, S.S., Anderson, J.B., Domack, E.W., 1999. Late Pleistocene-Holocene retreat of the West Antarctic Ice-Sheet system in the Ross Sea: Part 1 – Geophysical results. *Geological Society of America Bulletin 111*, 1486-1516.

Shipp, S.S., Wellner, J.A., Anderson, J.B., 2002. Retreat signature of a polar ice stream: Sub-glacial geomorphic features and sediments from the Ross Sea, Antarctica. *In:* Dowdeswell, J.A., Ó Cofaigh, C.S. (Eds.), *Glacier-influenced sedimentation on high latitude continental margins.* London, UK, Geological Society of London, 277-304.

Shreve, R.L., 1972. Movement of water in glaciers. *Journal of Glaciology 11*, 205-214.

Siegert, M.J., Dowdeswell, J.A., 2002. Late Weichselian iceberg, meltwater and sediment production from the Eurasian Ice Sheet: results from numerical ice sheet modelling. *Marine Geology 188*, 109-127.

Smith, A.M.T., Murray, K.W., Nicholls, K., Makinson, G., Aoalgeirsdottir, A.E.B., Vaughan, D.G., 2007. Rapid erosion, drumlin formation, and changing hydrology beneath an Antarctic ice stream. *Geology 35*, 127–130.

Smith, A.M., Murray, T., 2009. Bedform topography and basal conditions beneath a fast-flowing West Antarctic ice stream. *Quaternary Science Reviews 28*, 584–596.

Smith, J.A., Hillenbrand, C.-D., Kuhn, G., Larter, R.D., Graham, A.G.C., Ehrmann, W., Moreton, S.G., Forwick, M., 2011. Deglacial history of the West Antarctic Ice Sheet in the western Amundsen Sea Embayment. *Quaternary Science Reviews 30*, 488-505.

Smith, N.D., 1990. The effects of glacial surging on sedimentation in a modem ice-contact lake, Alaska. *Geological Society of America Bulletin 102*, 1393-1403.

Solheim, A., Pfirman, S.L., 1985. Sea-floor morphology outside a grounded, surging glacier: Bråsvellbreen, Svalbard. *Marine Geology 65*, 127-143.

Stoker, M.S., Holmes, R., 1991. Submarine end-moraines as indicators of Pleistocene ice-limits off Northwest Britain. *Journal of the Geological Society of London 148*, 431-434.

Stokes, C.R., Clark, C.D., Darby, D.A., Hodgson, D., 2005. Late Pleistocene ice export events into the Arctic Ocean from the M'Clure Strait Ice Stream, Canadian Arctic Archipelago. *Global and Planetary Change 49*, 139–162.

Svendsen, J.I., Mangerud, J., Elverhøi, A., Solheim, A., Schüttenhelm, R.T.E., 1992. The Late Weichselian glacial maximum on western Spitsbergen inferred from offshore sediment cores. *Marine Geology 104*, 1-17.

Svendsen, J.I., Elverhøi, A., Mangerud, J., 1996. The retreat of the Barents Sea Ice Sheet on the western Svalbard margin. *Boreas 25*, 244-256.

Svendsen, J.I., Alexanderson, H., Astakhov, V.I., Demidov, I., Dowdeswell, J.A., Funder, S., Gataullin, V., Henriksen, M., Hjort, C., Houmark-Nielsen, M., Hubberten, H.W., Ingólfsson, Ó., Jakobsson, M., Kjær, K.H., Larsen, E., Lokrantz, H., Lunkka, J.P., Lyså, A., Mangerud, J., Matiouchkov, A., Murray, A., Möller, P., Niessen, F., Nikolskaya, O., Polyak, L., Saarnisto, M., Siegert, C., Siegert, M.J., Spielhagen, R.F., Stein, R., 2004. Late Quaternary ice sheet history of northern Eurasia. *Quaternary Science Reviews 23*, 1229-1271.

Syvitski, J.P.M., 1989. On the deposition of sediment within glacier-influenced fjords: oceanographic controls. *Marine Geology 85*, 301-329.

Taylor, J., Dowdeswell, J.A., Siegert, M.J., 2002. Late Weichselian depositional processes, fluxes, and sediment volumes on the margins of the Norwegian Sea (62-75°N). *Marine Geology 188*, 61-77.

Todd, B.J., Page, V.C., Longva, O., Shaw, J., 2007. Glacial landforms on German Bank, Scotian Shelf: Evidence for Late Wisconsinan ice-sheet dynamics and implications for the formation of De Geer moraines. *Boreas 36*, 148–169.

Vanneste, L.E., Larter, R.D., 1995. Deep-tow boomer survey on the Antarctic Peninsula Pacific margin: an investigation of the morphology and acoustic characteristics of late Quaternary sedimentary deposits on the outer continental shelf and upper slope. *In:* Cooper, A.K., et al. (Eds.), *Geology and Seismic Stratigraphy of the Antarctic Margin,* Antarctic Research Series 68. AGU, Washington, D. C, pp. 97-121.

Vaughan, D.G., Doake, C.S.M., 1996. Recent atmospheric warming and retreat of ice shelves on the Antarctic Peninsula. *Nature 379*, 328–331.

Venteris, E.R., 1999. Rapid tidewater glacier retreat: a comparison between Columbia Glacier, Alaska and Patagonian calving glaciers. *Global and Planetary Change 22*, 131-138.

Vorren, T.O., Plassen, L., 2002. Deglaciation and palaeoclimate of the Andfjord-Vågsfjord area, North Norway. *Boreas 31*, 97–125.

Vorren, T.O., Laberg, J.S., Blaume, F., Dowdeswell, J.A., Kenyon, N.H., Mienert, J., Rumohr, J., Werner, F., 1998. The Norwegian–Greenland Sea continental margins: morphology and late Quaternary sedimentary processes and environment. *Quaternary Science Reviews 17*, 273–302.

Weertman, J., 1974. Stability of the junction of an ice sheet and an ice shelf. *Journal of Glaciology 13*, 3-11.

Whillans, I.M., van der Veen, C.J., 1997. The role of lateral drag in the dynamics of ice stream B, Antarctica. *Journal of Glaciology 43*, 231-237.

Winkelmann, D., Jokat, W., Jensen, L., Schenke, H.-W., 2010. Submarine end moraines on the continental shelf off NE Greenland - implications for Late glacial dynamics. *Quaternary Science Reviews 29*, 1069-1077.

Winsborrow, M.C.M., Clark, C.D., Stokes, C.R., 2010. What controls the location of ice streams? *Earth-Science Reviews 103*, 45–59.

Winsborrow, M.C.M., Stokes, C.R., Andreassen, K., 2012. Ice-stream flow switching during deglaciation of the southwestern Barents Sea. *Geological Society of American Bulletin 124*, 275-290.

9. FIGURE CAPTIONS

Figure 1. A: Schematic diagram of the position of the grounding zone at the margin of an ice sheet with a floating ice shelf. B: Schematic diagram of the position of the grounding zone at a tidewater ice-sheet margin. C: Typical ice-stream landform assemblage produced by fast, ice-stream flow on a continental margin (adapted from Ottesen and Dowdeswell, 2009). D: Typical inter-ice stream landform assemblage produced by slow-flowing ice on a continental margin (adapted from Ottesen and Dowdeswell, 2009). MSGL = mega-scale glacial lineations. GZW = grounding-zone wedge.

Figure 2. Landforms produced at the grounding zone of marine-terminating ice sheets. White arrows show inferred former ice-flow direction. A: Plan-view of a GZW in Vestfjorden, Norwegian margin (adapted from Ottesen et al., 2005b). The ice-distal side of the wedge is marked by the white dashed line. The wedge is overprinted by MSGL. B: Plan-view of a terminal-moraine ridge offshore of Nordaustlandet, Svalbard (adapted from Ottesen and Dowdeswell, 2006). The linear to curvilinear scours on the ridge are iceberg keel ploughmarks. Rhombohedral ridges are present on the ice-proximal side of the moraine ridge. C: Plan-view of a hummocky-terrain belt at the shelf break off northwest Svalbard (adapted from Ottesen and Dowdeswell, 2009). D: Plan-view of small retreat moraines in Borebukta, Svalbard (adapted from Ottesen and Dowdeswell, 2006). E: Schematic models of an ice-proximal fan formed under moderate meltwater discharge and high sediment discharge (adapted from Powell, 1990).

Figure 3. Map showing approximate GZW locations in the High Arctic, as determined from available bathymetric and acoustic data, overlying IBCAO bathymetry data (Jakobsson et al., 2012b). Red and blue circles are locations of surface and buried GZWs, respectively. Numbers refer to corresponding GZWs and references in Table 2. Red line is maximum ice-sheet extent during the Last Glacial Maximum (North American, Laurentide Ice Sheet is from Dyke et al., 2002; Eurasian Ice Sheet is from Svendsen et al., 2004; Greenland Ice Sheet is from Ehlers and Gibbard, 2007). A dashed line indicates uncertainty in the maximum ice position. Black lines delimit cross-shelf troughs in which GZWs are present. A: GZW locations in Arctic Canada. B: GZW locations on the Barents Sea and Norwegian margins. C: GZW locations off Greenland (GZW locations off northwest and northeast Greenland are determined from newly-available seismic reflection data provided by TGS). CAA = Canadian Arctic Archipelago; S = Svalbard.

Figure 4. Map showing approximate GZW locations in Antarctica, as determined from available bathymetric and acoustic data, overlying IBCAO bathymetry data (Jakobsson et al., 2012b). Red circles are approximate locations of surface GZWs. Black lines delimit cross-shelf troughs in which GZWs are present. The numbers refer to the corresponding GZW and references in Table 2. The red line is the maximum extent of the Antarctic Ice Sheet at the last glacial maximum (from Livingstone et al., 2012). A dashed line indicates uncertainty in the maximum ice position. Black lines delimit cross-shelf troughs in which GZWs are present. A: GZW locations off the Antarctic Peninsula, in the Bellingshausen Sea and in the Amundsen Sea. B: GZW locations in the Ross Sea and in Mertz Trough, East Antarctica. C: GZW locations in Prydz Channel, Nielsen Basin and Iceberg Alley Trough, East Antarctica.

Figure 5. A: High-latitude GZW lengths, coloured by margin, as determined from available accounts of Arctic and Antarctic GZWs. B: Histogram of GZW lengths on the Greenland margin. C: Histogram of GZW lengths on the Antarctic margin.

Figure 6. A: High-latitude GZW maximum thicknesses, coloured by margin, as determined from available accounts of Arctic and Antarctic GZWs. B: Histogram of GZW maximum thicknesses on the Greenland margin. C: Histogram of GZW maximum thicknesses on the Antarctic margin.

Figure 7. High-latitude GZW dimensions, coloured by margin, as determined from available accounts of Arctic and Antarctic GZWs. 'C' is shown next to GZWs that have been interpreted as composite landforms formed during multiple ice advances. A: Scatter-plot of the relationship between GZW length and thickness. B: Scatter-plot with linear regression of the relationship between GZW length and thickness, omitting GZWs off Antarctica. C: Scatter-plot with linear regression of the relationship between GZW length and thickness for GZWs on the Greenland and Antarctic margins.

Figure 8. Examples of GZWs on seismic profiles from high-latitude continental margins. A: Buried GZW in Amundsen Gulf Trough, Canadian Beaufort Sea (no. 2 in Fig. 3A and Table 2) (adapted from Batchelor et al., 2014). Vertical exaggeration (VE) = 30. Yellow line is GZW outline. B: Surface GZW in Norske Trough, Northeast Greenland (no. 58 in Fig. 3C and Table 2). VE = 30. C: Large, possibly composite GZW in Prydz Channel Trough, East Antarctica (no. 134 in Fig. 4C and Table 2) (adapted from O'Brien et al., 1999). VE = 20. Twt is two-way travel time. A velocity of 1500 m/s was used to calculate the approximate depth scale. D: Small outer-shelf GZW in Melville Bugt Trough, Northwest Greenland (no.

49 in Fig. 3C and Table 2). VE = 12. E: GZW on the outermost shelf of Melville Bay Trough, Northwest Greenland (no. 45 in Fig. 3C and Table 2). VE = 17. F: Topographically-controlled GZW on a bedrock high in an unnamed trough, Northwest Greenland (no. 39 in Figs. 3C and Table 2). VE = 17. Yellow line is basal reflection of wedge in B to F. Seismic reflection data in B and D to F is provided by TGS.

Figure 9. Seismic examples of GZWs formed at the outer-shelf lateral margins of high-latitude cross-shelf troughs, overlying IBCAO bathymetry data (Jakobsson et al., 2012b). A: GZW formed at the southern lateral margin of an unnamed trough off Northwest Greenland (no. 53 in Fig. 3C and Table 2). VE = 32. Seismic reflection data provided by TGS. B: IBCAO sea floor bathymetry (50 m contours; Jakobsson et al., 2012) of an unnamed trough off Northwest Greenland, showing the location of the seismic profile in A. C: GZW formed at the northern lateral margin of the Amundsen Gulf Trough, Canadian Beaufort Sea margin (no. 3 in Fig. 3A and Table 2) (adapted from Batchelor et al., 2014). VE = 55. D: GZW formed at the southern lateral margin of the M'Clure Strait Trough, Canadian Beaufort Sea margin (no. 4 in Fig. 3A and Table 2) (adapted from Batchelor et al., 2014). VE = 45. E: IBCAO sea floor bathymetry (50 m contours; Jakobsson et al., 2012) of the Amundsen Gulf and M'Clure Strait troughs on the Canadian Beaufort Sea margin, showing the locations of the seismic profiles in C and D. Yellow line is basal reflection of GZWs in A, C and D. Dashed yellow lines are horizons onto which internal reflections downlap, suggesting several different phases of wedge formation.

Figure 10. A: Schematic model of an idealised cross-shelf trough with a GZW formed at a vertical pinning point. B: IBCAO bathymetry (Jakobsson et al., 2012b) of an unnamed trough off northwest Greenland, showing the location of seismic profile b – b' through a GZW

formed at a vertical pinning point (no. 39 in Fig. 3C). Seismic profile b – b' is from newly-available seismic data provided by TGS. C: Schematic model of an idealised cross-shelf trough with a GZW formed at a lateral pinning point. D: IBCAO bathymetry of Kongsfjorden Trough on the western Barents Sea margin, showing the location of sparker profile d – d' through a GZW formed at a lateral pinning point (no. 12 in Fig. 3B). Sparker profile d - d' is adapted from Ottesen et al., 2007. E: Schematic model of an idealised cross-shelf trough with a GZW formed on the outermost continental shelf. F: IBCAO bathymetry of Kveithola Trough on the western Barents Sea margin, showing the location of CHIRP profile f – f' through a GZW formed on the outermost continental shelf (no. 18 in Fig. 3B). CHIRP profile f – f' is adapted from Rebesco et al., 2011. G: Schematic model of an idealised cross-shelf trough with a GZW formed at the outer-shelf lateral margin. H: IBCAO bathymetry of Amundsen Gulf Trough on the Canadian Beaufort Sea margin, showing the location of seismic profile h – h' through a GZW formed at the outer-shelf lateral margin of the trough (no. 3 in Fig. 3A). Seismic profile h – h' is adapted from Batchelor et al., 2014.

Figure 11. Diagram illustrating the factors controlling the formation of GZWs on high-latitude continental margins.

Table 1. List of ice-marginal landforms produced at the grounding zone of marine-terminating ice sheets and glaciers, together with the terminologies that have been assigned previously to them.

Table 2. The dimensions and characteristics of grounding-zone wedges on high-latitude continental margins, as determined from available accounts of Arctic and Antarctic cross-shelf troughs. Type 1, 2, 3 and 4 GZWs have been interpreted to have developed at vertical

pinning points, at lateral pinning points, on the outermost continental shelf, and at the outer-shelf lateral margins, respectively. *Thickness is maximum grounding-zone wedge thickness.

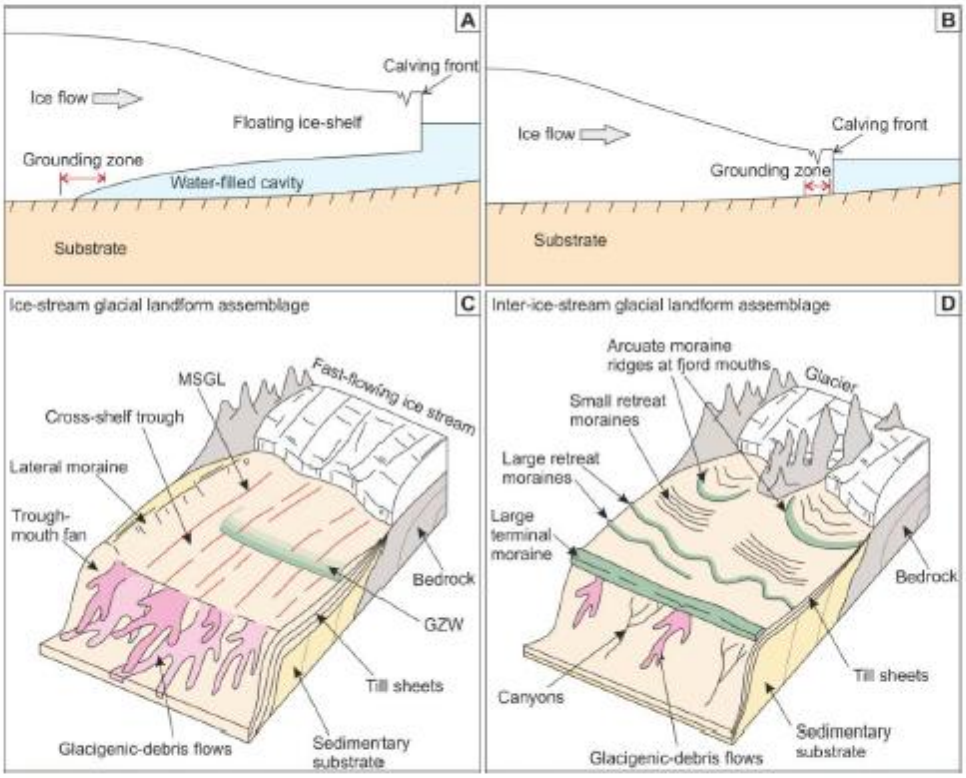
A
Calving front
Ice flow
Floating ice-shelf
Grounding zone
Water-filled cavity
Substrate
B
Ice flow
Calving front
Grounding zone
Substrate
Ice-stream glacial landform assemblage
C
Fast-flowing ice stream
MSGL
Cross-shelf trough
Lateral moraine
Trough-
mouth fan
Bedrock
GZW
Till sheets
Glacigenic-debris flows
Sedimentary
substrate
Inter-ice-stream glacial landform assemblage
D
Arcuate moraine
ridges at fjord mouths
Glacier
Small retreat
moraines
Large retreat
moraines
Large
terminal
moraine
Bedrock
Till sheets
Canyons
Sedimentary
substrate
Glacigenic-debris flows

Fig. 1

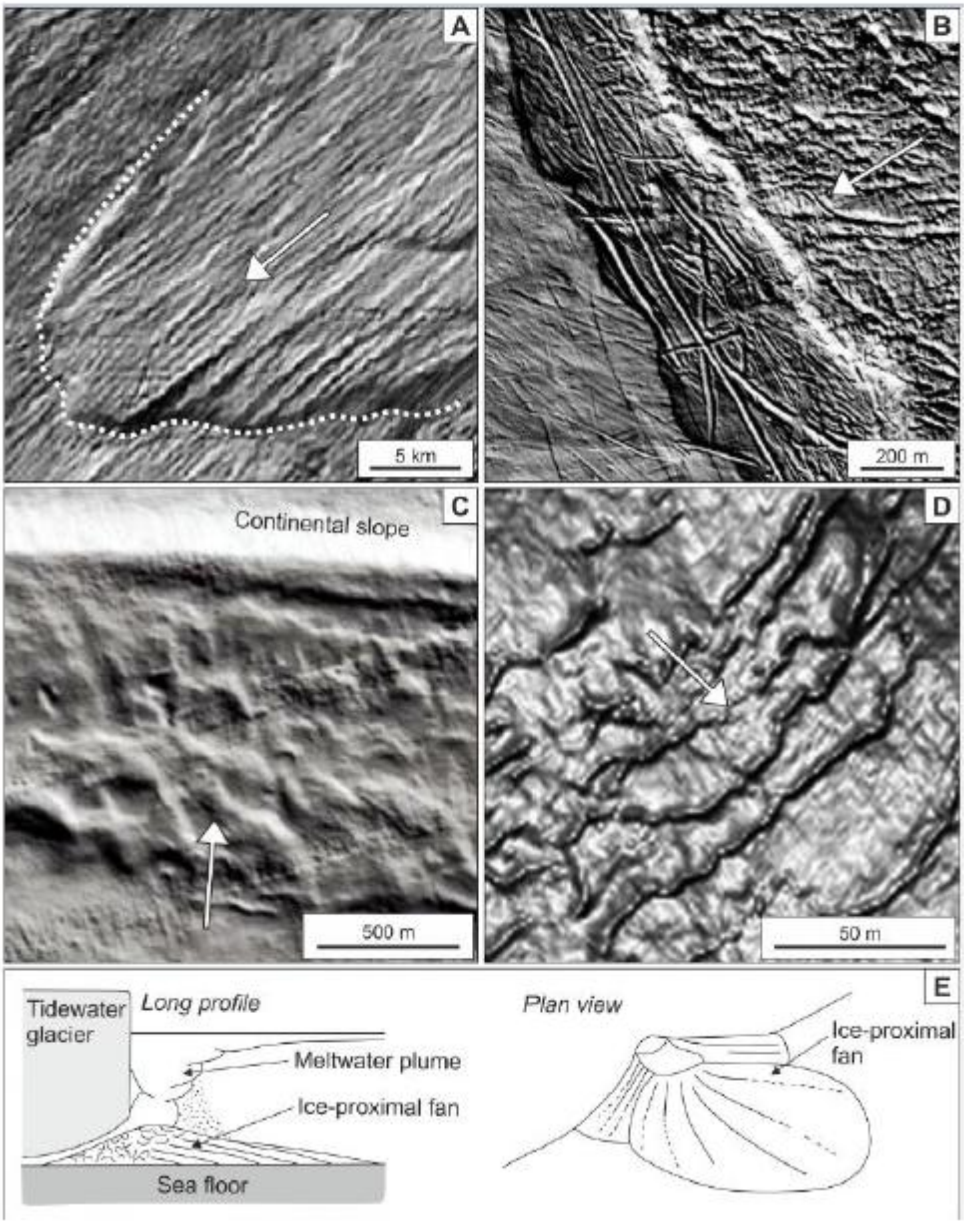
A
5 km
B
200 m
C
Continental slope
500 m
D
50 m
E
Tidewater glacier
Long profile
Meltwater plume
Ice-proximal fan
Sea floor
Plan view
Ice-proximal fan

Fig. 2

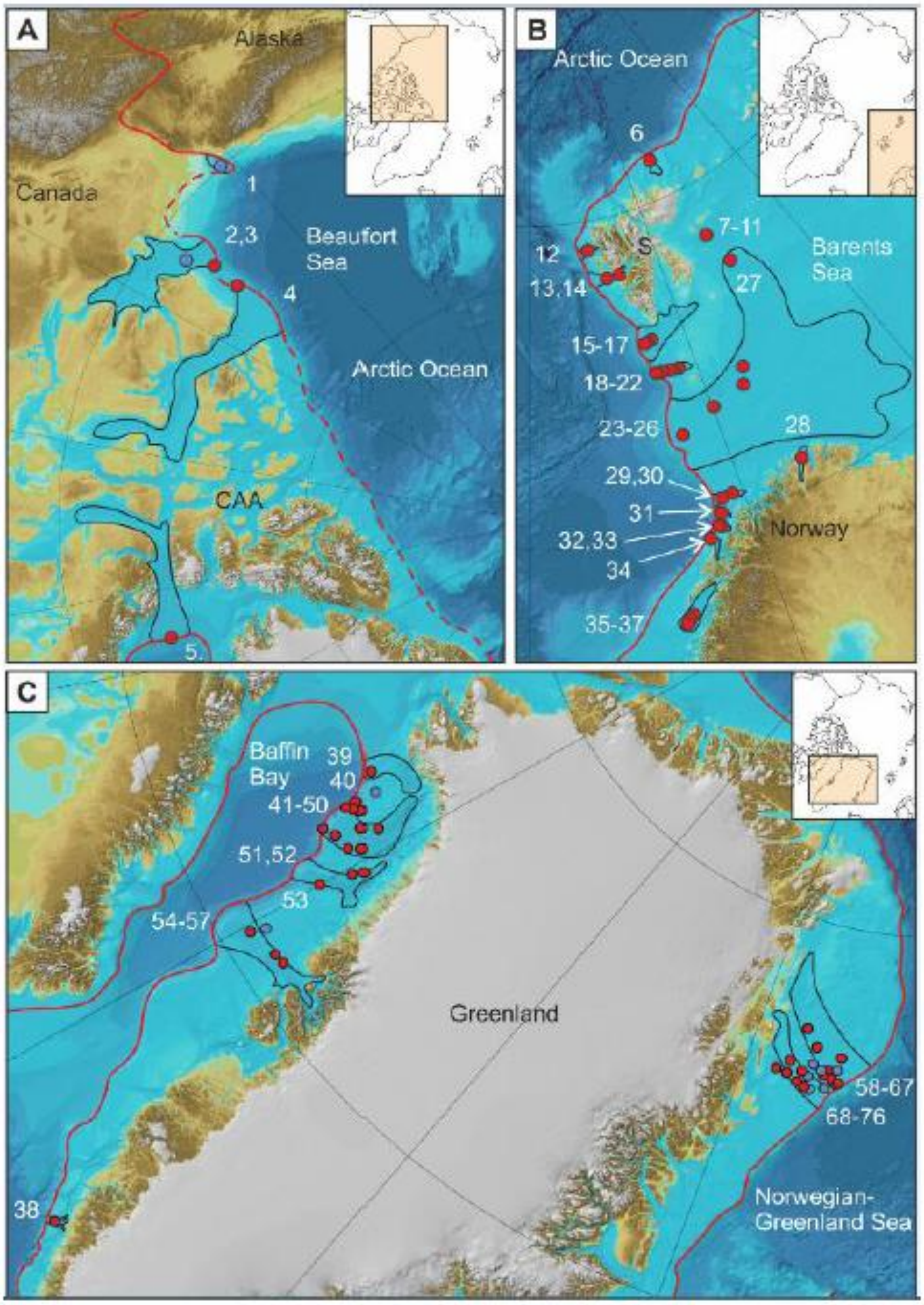
A
Alaska
Canada
1
2,3
Beaufort
Sea
4
Arctic Ocean
CAA
5
B
Arctic Ocean
6
7-11
12
S
13,14
Barents
Sea
27
15-17
18-22
23-26
28
29,30
31
32,33
34
Norway
35-37
C
Baffin
Bay
39
40
41-50
51,52
53
54-57
Greenland
58-67
68-76
38
Norwegian-
Greenland Sea

Fig. 3

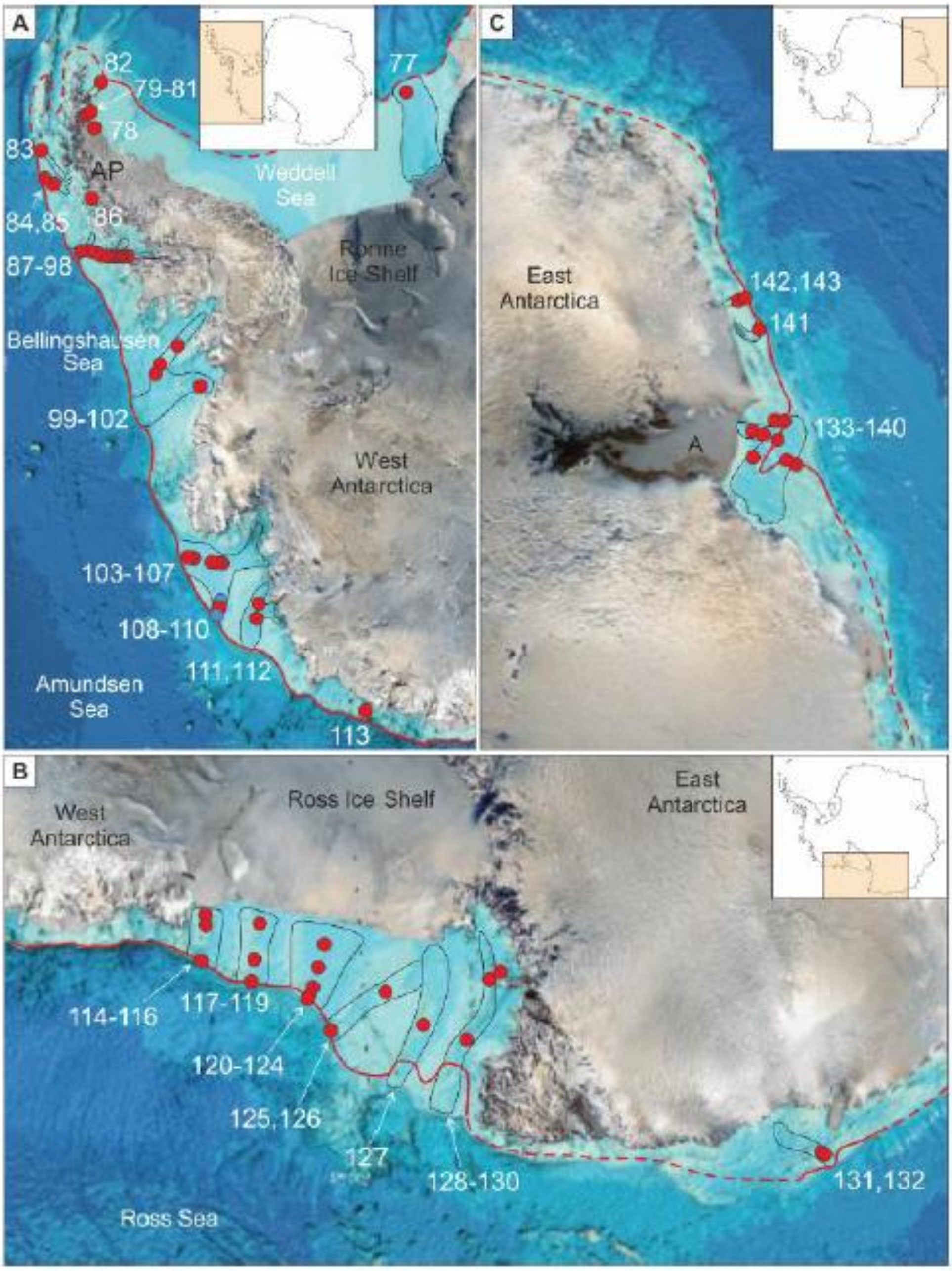
A
82
79-81
78
83
AP
84,85
86
87-98
77
Weddell
Sea
Ronne
Ice Shelf
Bellingshausen
Sea
99-102
West
Antarctica
103-107
108-110
111,112
Amundsen
Sea
113
C
East
Antarctica
142,143
141
133-140
A
B
West
Antarctica
Ross Ice Shelf
East
Antarctica
114-116
117-119
120-124
125,126
127
128-130
131,132
Ross Sea

Fig. 4

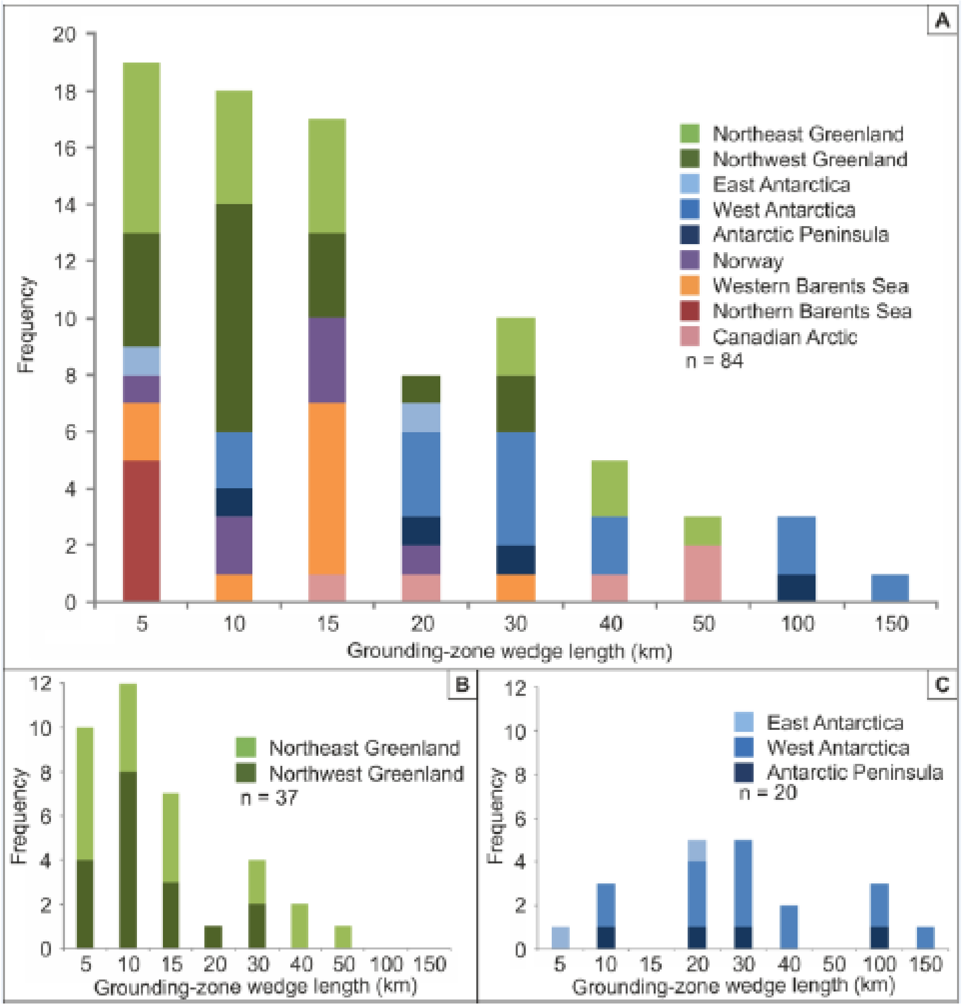
A
Frequency
Grounding-zone wedge length (km)
Northeast Greenland
Northwest Greenland
East Antarctica
West Antarctica
Antarctic Peninsula
Norway
Western Barents Sea
Northern Barents Sea
Canadian Arctic
n = 84
B
Northeast Greenland
Northwest Greenland
n = 37
C
East Antarctica
West Antarctica
Antarctic Peninsula
n = 20

Fig. 5

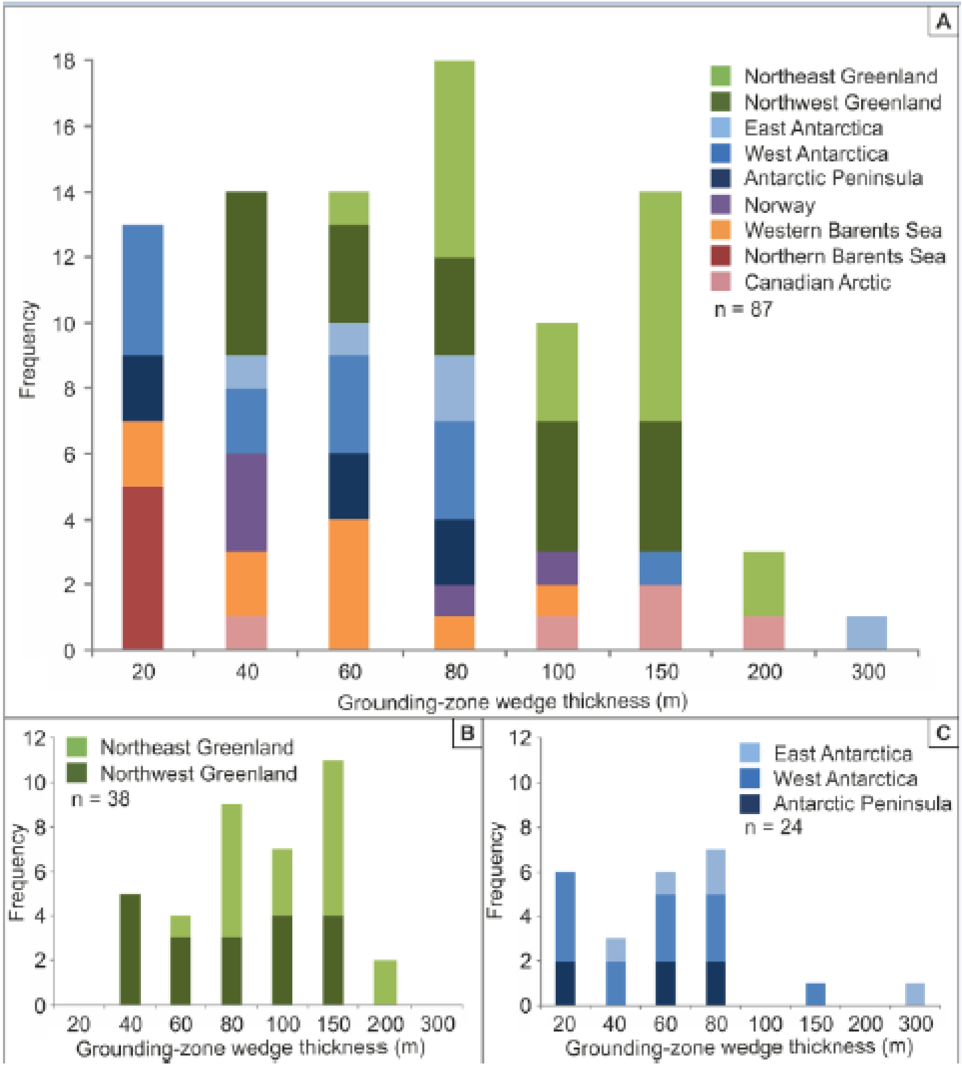
A
Frequency
Grounding-zone wedge thickness (m)
Northeast Greenland
Northwest Greenland
East Antarctica
West Antarctica
Antarctic Peninsula
Norway
Western Barents Sea
Northern Barents Sea
Canadian Arctic
n = 87
B
Frequency
Grounding-zone wedge thickness (m)
Northeast Greenland
Northwest Greenland
n = 38
C
Frequency
Grounding-zone wedge thickness (m)
East Antarctica
West Antarctica
Antarctic Peninsula
n = 24

Fig. 6

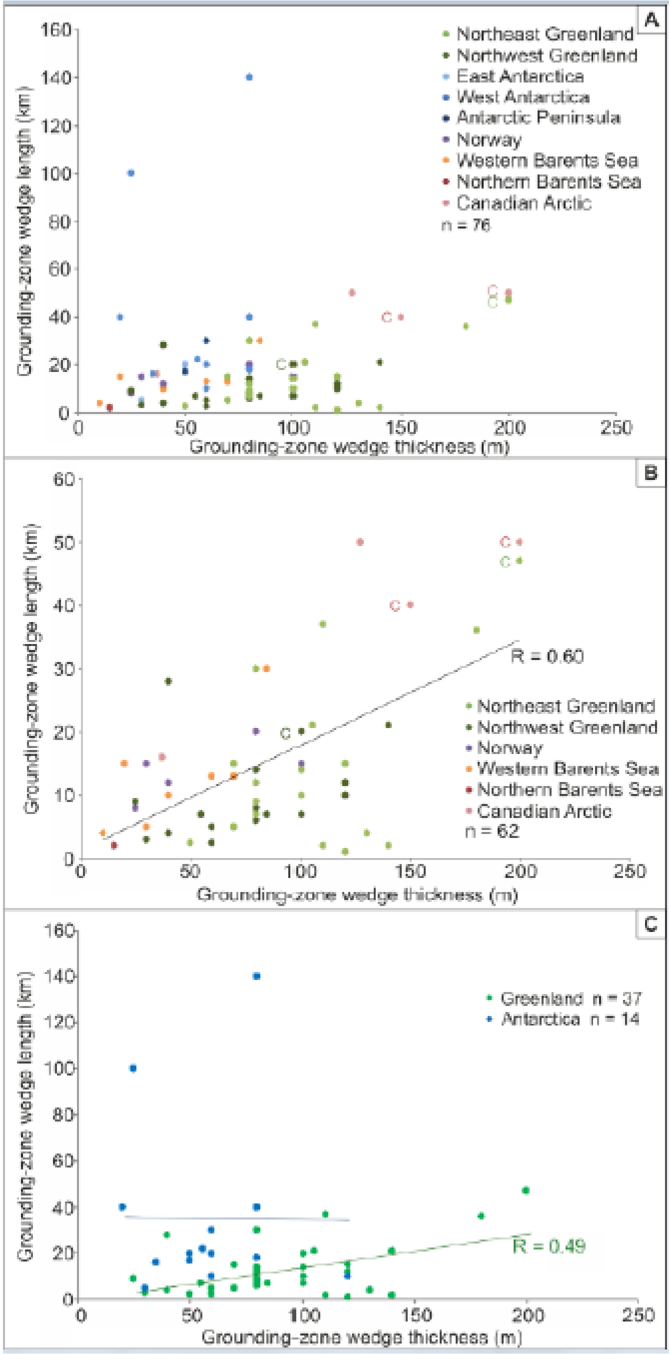
A
Northeast Greenland
Northwest Greenland
East Antarctica
West Antarctica
Antarctic Peninsula
Norway
Western Barents Sea
Northern Barents Sea
Canadian Arctic
n = 76
Grounding-zone wedge length (km)
Grounding-zone wedge thickness (m)
B
R = 0.60
Northeast Greenland
Northwest Greenland
Norway
Western Barents Sea
Northern Barents Sea
Canadian Arctic
n = 62
Grounding-zone wedge length (km)
Grounding-zone wedge thickness (m)
C
Greenland n = 37
Antarctica n = 14
R = 0.49
Grounding-zone wedge length (km)
Grounding-zone wedge thickness (m)

Fig. 7

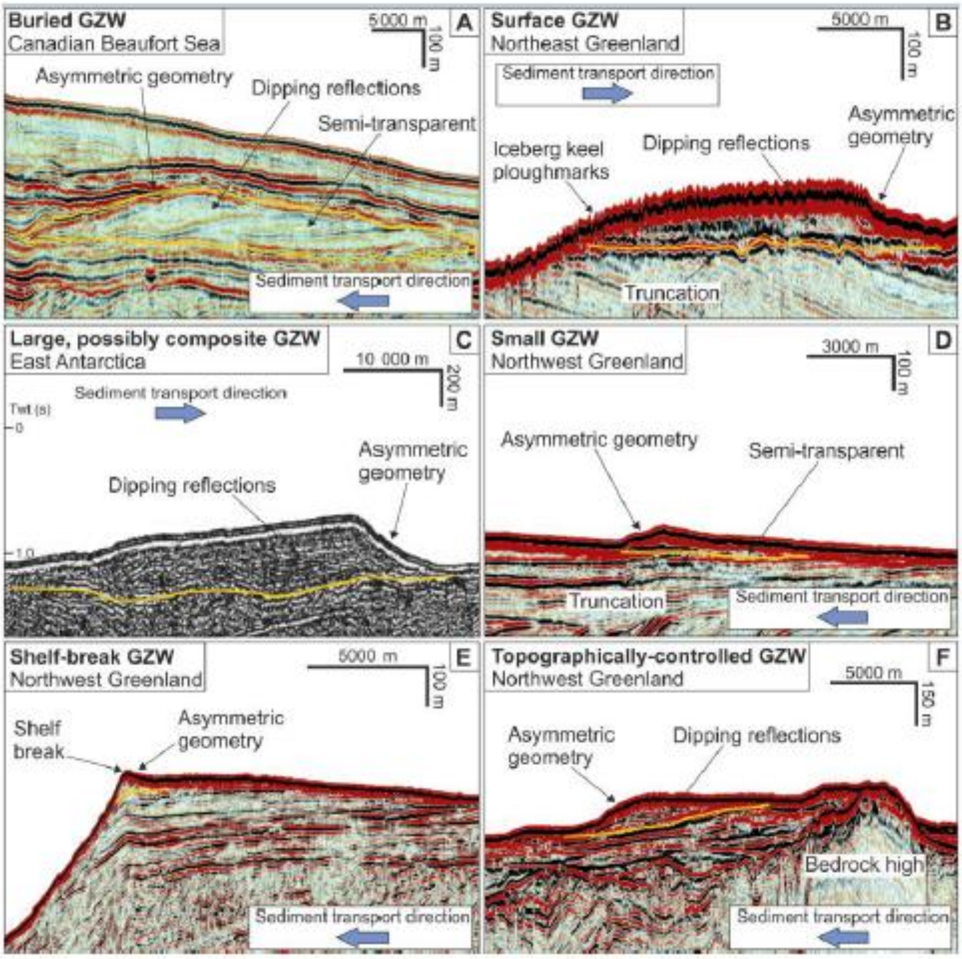

Buried GZW
Canadian Beaufort Sea
5000 m
100 m
A
Asymmetric geometry
Dipping reflections
Semi-transparent
Sediment transport direction
Surface GZW
Northeast Greenland
5000 m
100 m
B
Sediment transport direction
Asymmetric geometry
Iceberg keel ploughmarks
Dipping reflections
Truncation
Large, possibly composite GZW
East Antarctica
C
10 000 m
200 m
Sediment transport direction
Twt (s)
0
1.0
Asymmetric geometry
Dipping reflections
Small GZW
Northwest Greenland
3000 m
100 m
D
Asymmetric geometry
Semi-transparent
Truncation
Sediment transport direction
Shelf-break GZW
Northwest Greenland
5000 m
100 m
E
Shelf break
Asymmetric geometry
Sediment transport direction
Topographically-controlled GZW
Northwest Greenland
5000 m
150 m
F
Asymmetric geometry
Dipping reflections
Bedrock high
Sediment transport direction

Fig. 8

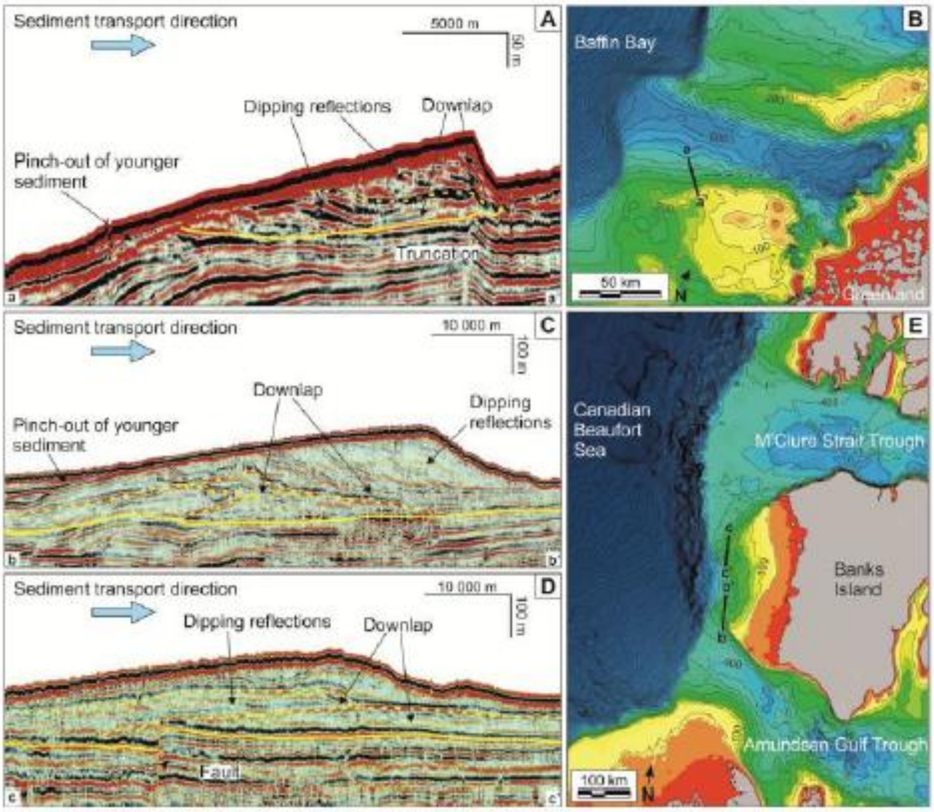
Sediment transport direction
5000 m
50 m
A
Dipping reflections
Downlap
Pinch-out of younger sediment
Truncation
B
Baffin Bay
50 km
N
Greenland
Sediment transport direction
10 000 m
100 m
C
Downlap
Dipping reflections
Pinch-out of younger sediment
E
Canadian Beaufort Sea
M'Clure Strait Trough
Banks Island
Amundsen Gulf Trough
100 km
Sediment transport direction
10 000 m
100 m
D
Dipping reflections
Downlap
Fault

Fig. 9

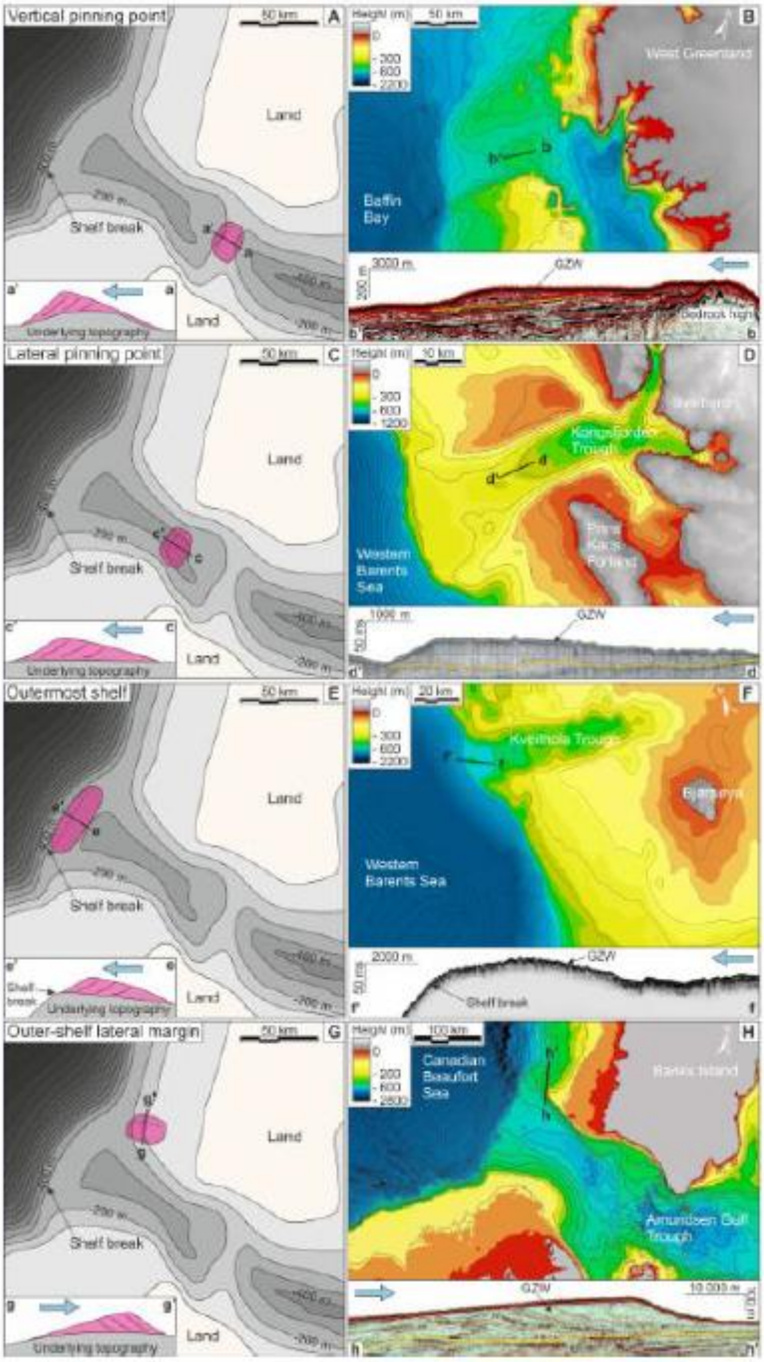
Vertical pinning point
A
Land
Shelf break
Underlying topography
B
West Greenland
Baffin Bay
GZW
Bedrock high
Lateral pinning point
C
D
Kongsfjorden Trough
Western Barents Sea
Prins Karls Forland
Outermost shelf
E
F
Kveithola Trough
Bjørnøya
Western Barents Sea
Shelf break
Outer-shelf lateral margin
G
H
Canadian Beaufort Sea
Banks Island
Amundsen Gulf Trough

Fig. 10

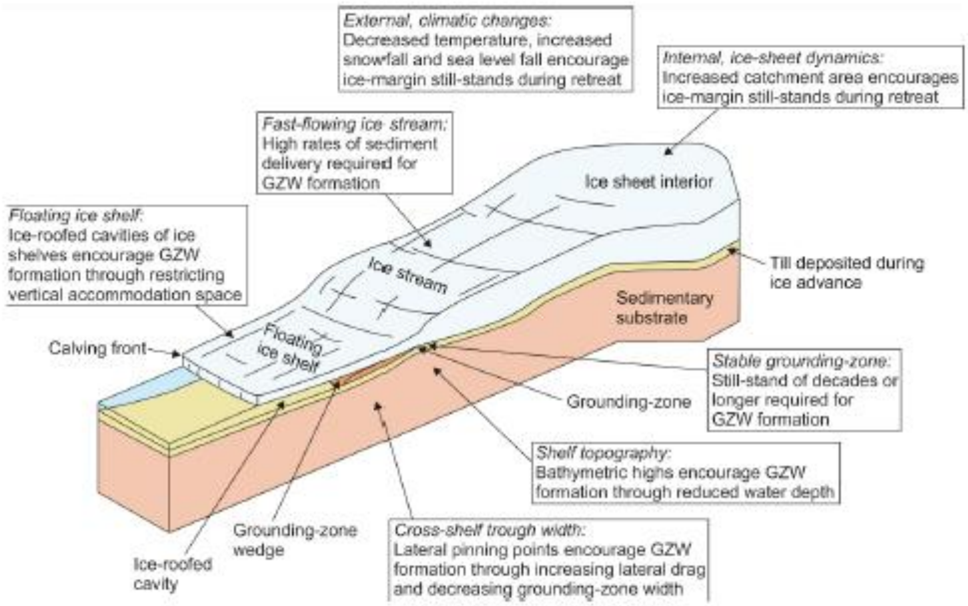
External, climatic changes:
Decreased temperature, increased snowfall and sea level fall encourage ice-margin still-stands during retreat
Internal, ice-sheet dynamics:
Increased catchment area encourages ice-margin still-stands during retreat
Fast-flowing ice stream:
High rates of sediment delivery required for GZW formation
Ice sheet interior
Floating ice shelf:
Ice-roofed cavities of ice shelves encourage GZW formation through restricting vertical accommodation space
Ice stream
Till deposited during ice advance
Sedimentary substrate
Floating ice shelf
Calving front
Stable grounding-zone:
Still-stand of decades or longer required for GZW formation
Grounding-zone
Shelf topography:
Bathymetric highs encourage GZW formation through reduced water depth
Grounding-zone wedge
Cross-shelf trough width:
Lateral pinning points encourage GZW formation through increasing lateral drag and decreasing grounding-zone width
Ice-roofed cavity

Fig. 11

Table 1

Landform description	Terminologies	References
Asymmetric wedge	Grounding-zone wedge	Bart and Anderson, 1997; Dowdeswell and Fugelli, 2012; **this study**
	Grounding-line wedge	Powell, 1991; Powell and Domack, 1995; Powell and Alley, 1997
	Till delta	Alley et al., 1987; Larter and Vanneste, 1995
Moraine ridge	Submarine moraine (terminal/ recessional/ lateral)	Powell, 1981; Holtedahl, 1989; Ottesen et al., 2007
Fan	Ice-proximal fan	Dowdeswell et al., Submitted; **this study**
	Subaqueous outwash fan	Retelle and Bither, 1988
	Grounding-line fan	Powell, 1990; Lønne, 1997; Seramur et al., 1997
	Glacier-contact fan	Boulton, 1986
	Subaqueous fan	Ashley et al., 1991
Sheet	Till sheet	Powell, 1981, 1984; Shipp et al., 1999
	Till tongue	King and Fader, 1986; King et al., 1987, 1991

Table 2

No.	Location	Position	Length (km)	Width (km)	Thickness (m) *	Acoustic character	Chronology	Type	References
Canadian Arctic									
1.	Mackenzie Trough	Mid/ outer-shelf	14	25	100	Low-amplitude stratified reflections	Buried	1. Vert.	Batchelor et al., 2013a, b
2.	Amundsen Gulf Trough	Middle-shelf	50	30	127	Semi-transparent, low-amplitude dipping reflections	Buried	2. Lat.	Batchelor et al., 2013a, 2014
3.	Amundsen Gulf Trough	Outer-shelf lateral margin	50		200	Semi-transparent, low-amplitude dipping reflections	Surface Composite	4. Marg.	Batchelor et al., 2013a, 2014
4.	M'Clure Strait Trough	Outer-shelf lateral margin	40		150	Semi-transparent, low-amplitude dipping reflections	Surface Composite	4. Marg.	Batchelor et al., 2013a, 2014
5.	Lancaster Sound Trough	7 wedges on outer-most shelf	16 (largest wedge)		37	Transparent with rare dipping reflections and erosional base	Surface		Li et al., 2011
Northern Barents Sea									
6.	Albertini Trough	Outer-shelf					Surface		Noormets et al., 2012
7-11.	Olga Strait	Barents Sea	2		10 - 15	Transparent	Surface		Hogan et al., 2010
Western Barents Sea									
12.	Kongsfjorden	Mid-shelf	5		30	Transparent	Surface	2. Lat.	Ottesen et al., 2005a, 2007
13.	Isfjorden	Mid-shelf	10		40		Surface	2. Lat.	Svendsen et al., 1992, 1996; Ottesen et al., 2005a, 2007
14.	Grønfjorden	Outer-fjord/ inner-shelf	4		10	Transparent	Surface	1. Vert.	Forwick and Vorren, 2011
15-17.	Storfjorden	3 wedges on mid/ outer-shelf					Surface 16.3 – 10 ka (C14)		Pedrosa et al., 2011; Lucchi et al., 2012
18.	Kveithola Trough	Outer-most shelf	10 - 13		70	Transparent	Surface	3. Outer-most shelf	Rebesco et al., 2011; Bjarnadóttir et al., 2013
19.	Kveithola Trough	Outer-shelf	10 - 13		30 - 60	Transparent	Surface	2. Lat.	Rebesco et al., 2011; Bjarnadóttir et al., 2013
20.	Kveithola Trough	Mid-shelf	10 - 13		30 - 60	Transparent	Surface		Rebesco et al., 2011; Bjarnadóttir et al., 2013
21.	Kveithola Trough	Mid-shelf	10 - 13		30 - 60	Transparent	Surface		Bjarnadóttir et al., 2013

22.	Kveithola Trough	Mid-shelf	10 - 13		30 - 60	Transparent	Surface		Bjarnadóttir et al., 2013
23.	Bear Island Trough	Outer-shelf	30	280	85	Transparent to chaotic	Surface 17.1 – 17.6 ka	1. Vert.	Andreassen et al., 2008; Winsborrow et al., 2010; Rüther et al., 2011
24.	Bear Island Trough	Mid-shelf					Surface		Andreassen et al., 2008; Winsborrow et al., 2010
25.	Bear Island Trough	Inner-shelf					Surface		Andreassen et al., 2008; Winsborrow et al., 2010
26.	Bear Island Trough	Inner-shelf					Surface		Andreassen et al., 2008; Winsborrow et al., 2010
27.	Bear Island Trough	Inner-shelf	15	66	20	Transparent	Surface		Andreassen et al., 2014
Norwegian Margin									
28.	Porsangerfjor-den	Outer-fjord/ inner-shelf	10				Surface	2. Lat.	Ottesen et al., 2008; Winsborrow et al., 2010
29.	Håkjerringdju-pet	Outer-shelf	12		40		Surface	2. Lat.	Ottesen et al., 2008; Winsborrow et al., 2010, 2012
30.	Håkjerringdju-pet	Outer-shelf	8		25		Surface	2. Lat.	Ottesen et al., 2008; Winsborrow et al., 2010, 2012
31.	Rebbenesedj-upet	Outer-shelf	15	16	30	Transparent	Surface	2. Lat.	Ottesen et al., 2008; Winsborrow et al., 2010; Rydningen et al., 2013
32.	Malangsdjup-et	Outer-most shelf				Transparent with dipping reflections	Surface	3. Outer-most shelf	Rydningen et al., 2013
33.	Malangsdjup-et	Outer-shelf	15	20	100	Transparent	Surface	2. Lat.	Ottesen et al., 2008; Rydningen et al., 2013
34.	Andfjorden (Egga moraines)	Outer-most shelf				Transparent with dipping reflections	Surface	3. Outer-most shelf	Vorren and Plassen, 2002; Ottesen et al., 2007; Rydningen et al., 2013
35.	Vestfjorden (Røst moraine/ Tennholmen Ridge)	Inner-trough	20	60	80	Transparent	Surface 16.2 ka		Ottesen et al., 2005a, b; Knies et al., 2007; Dowdeswell et al., 2008; Laberg et al., 2007, 2009
36.	Vestfjorden (Værøy moraine)	Inner-trough	5	30		Transparent	Surface 14.5 ka		Ottesen et al., 2005a, b; Knies et al.,

									2007; Dowdeswell et al., 2008; Laberg et al., 2007, 2009
37.	Vestfjorden (Salten moraine)	Inner-trough		20		Transparent	Surface < 16.2 ka		Ottesen et al., 2005a, b; Knies et al., 2007; Dowdeswell et al., 2008; Laberg et al., 2007, 2009
Southwest Greenland									
38.	Fiskenæs Trough	Mid-shelf					Surface		Ryan et al., In Press
Northwest Greenland									
39.	Unnamed Trough	Lateral, outer-shelf	10		120	Semi-transparent with dipping reflections	Surface	1. Vert.	Dowdeswell and Fugelli, 2012
40.	Inter-trough region of shelf		14		80	Semi-transparent with dipping reflections	Buried		Dowdeswell and Fugelli, 2012
41.	Melville Bay Trough	Lateral, outer-shelf	7		100	Semi-transparent	Surface		Dowdeswell and Fugelli, 2012
42.	Melville Bay Trough	Outer-shelf	7		55	Semi-transparent	Surface	1. Vert.	Dowdeswell and Fugelli, 2012
43.	Melville Bay Trough	Outer-shelf	5		60		Surface		Dowdeswell and Fugelli, 2012
44.	Melville Bay Trough	Outer-shelf	12		120	Dipping internal reflections	Surface		Dowdeswell and Fugelli, 2012
45.	Melville Bay Trough	Outer-most shelf	2.5		60	Semi-transparent with dipping reflections	Surface	3. Outer-most shelf	Dowdeswell and Fugelli, 2012
46.	Melville Bay Trough	Mid-shelf	7		85	Dipping internal reflections	Surface	1. Vert.	Dowdeswell and Fugelli, 2012
47.	Melville Bay Trough	Inner-shelf	3		30	Semi-transparent with truncation at base	Surface		
48.	Melville Bay Trough	Outer-shelf	8		80	Dipping internal reflections	Surface		Dowdeswell and Fugelli, 2012
49.	Melville Bay Trough	Outer-shelf	6		80		Surface		Dowdeswell and Fugelli, 2012
50.	Melville Bay Trough	Mid-shelf	4		40		Surface		
51.	Unnamed Trough	Inner-shelf	21		140	Semi-transparent with dipping internal reflections	Surface		Dowdeswell and Fugelli, 2012
52.	Unnamed Trough	Inner-shelf	7		100		Surface		Dowdeswell and Fugelli, 2012
53.	Unnamed Trough	Lateral outer-	15		120	Semi-transparent with	Surface	4. Marg.	Dowdeswell and Fugelli,

		shelf margin			dipping internal reflections			2012
54.	Uummannaq Trough	Inner-shelf		25		Surface	2. Lat.	Dowdeswell et al., 2014.
55.	Uummannaq Trough	Inner-shelf	9	25		Surface	2. Lat.	Dowdeswell et al., 2014.
56.	Uummannaq Trough	Mid-shelf	28	40		Surface		Dowdeswell et al., 2014.
57.	Uummannaq Trough	Lateral margin	20	100	Semi-transparent with dipping internal reflections	Buried Composite	4. Marg.	Dowdeswell and Fugelli, 2012
Northeast Greenland								
58.	Norske Trough	Mid-shelf	21	105	Semi-transparent	Surface		Dowdeswell and Fugelli, 2012
59.	Norske Trough	Mid-shelf	47	200	Semi-transparent with dipping internal reflections	Surface Composite		Dowdeswell and Fugelli, 2012
60.	Norske Trough	Outer-shelf	36	180	Semi-transparent	Surface		Dowdeswell and Fugelli, 2012
61.	Norske Trough	Outer-most shelf	7	80	Semi-transparent with dipping internal reflections	Buried	3. Outer-most shelf	Dowdeswell and Fugelli, 2012
62.	Norske Trough	Mid-shelf	15	120	Semi-transparent	Buried		Dowdeswell and Fugelli, 2012
63.	Norske Trough	Outer-shelf	9	80	Semi-transparent	Buried		Dowdeswell and Fugelli, 2012
64.	Norske Trough	Outer-most shelf	4	130	Semi-transparent with dipping internal reflections	Surface	3. Outer-most shelf	Dowdeswell and Fugelli, 2012
65.	Norske Trough	Inner-shelf	14	100	Semi-transparent	Surface		Dowdeswell and Fugelli, 2012; Laberg et al., 2014
66.	Norske Trough	Middle-shelf	1	120	Semi-transparent	Surface		Dowdeswell and Fugelli, 2012
67.	Norske Trough	Outer-most shelf	2	140	Semi-transparent	Surface	3. Outer-most shelf	Dowdeswell and Fugelli, 2012; Laberg et al., 2014
68.	Store Koldewey Trough	Inner-shelf	12	80	Semi-transparent	Surface		Dowdeswell and Fugelli, 2012
69.	Store Koldewey Trough	Middle-shelf	2.5	50		Surface		Dowdeswell and Fugelli, 2012
70.	Store Koldewey Trough	Middle-shelf	37	110	Semi-transparent	Buried		Dowdeswell and Fugelli, 2012
71..	Store Koldewey Trough	Outer-shelf	30	80	Semi-transparent	Buried		Dowdeswell and Fugelli, 2012
72.	Store Koldewey Trough	Inner-shelf	10	100	Semi-transparent	Surface		Dowdeswell and Fugelli, 2012
73.	Store	Middle-	5	70	Semi-	Surface		Dowdeswell

	Koldewey Trough	shelf			transparent			and Fugelli, 2012
74.	Store Koldewey Trough	Middle-shelf	2	110	Semi-transparent	Surface		Dowdeswell and Fugelli, 2012
75.	Store Koldewey Trough	Middle-shelf	10	100	Semi-transparent	Surface		Dowdeswell and Fugelli, 2012
76.	Store Koldewey Trough	Middle-shelf	15	70	Semi-transparent	Buried		Dowdeswell and Fugelli, 2012
Antarctic Peninsula								
77.	Filchner Trough	Outer-shelf			Transparent	Surface		Larter et al., 2012
78.	Crane Fjord	Fjord mouth				Surface		Rebesco et al., 2014
79.	Northern Larsen A	Mid-shelf				Surface		Evans et al., 2005
80.	Prince Gustav Channel	Mid-shelf	80		Massive to chaotic, seaward-dipping downlapping reflections	Surface		Anderson, 1997, 1999; Anderson et al., 2002; Evans et al., 2005
81.	Shelf beyond Larsen Inlet	Mid-shelf				Surface		Gilbert et al., 2003; Evans et al., 2005
82.	Vega Trough	Outer-shelf		75		Surface Min. 18,410 cal yr BP		Anderson, 1997; Bentley and Anderson, 1998; Heroy and Anderson, 2005
83.	Boyd Strait	Outer-shelf		75		Surface	4. Marg	Vanneste and Larter, 1995
84.	Anvers Trough	Outer-shelf lateral margin	30	> 60	Low-amplitude dipping parallel to subparallel reflections	Surface	4. Marg.	Larter and Vanneste, 1995; Vanneste and Larter, 1995
85.	Anvers Trough	Mid-shelf	17	50		Surface		Vanneste and Larter, 1995
86.	Barilari Bay	Inner-shelf	8			Surface		Christ et al., 2014
87.	Marguerite Trough	Outer-shelf		> 20	Transparent with dipping reflections	Surface	2. Lat.	Bentley and Anderson, 1998; Ó Cofaigh et al., 2002, 2005a, 2008; Jamieson et al., 2012
88.	Marguerite Trough	Outer-shelf		> 20	Transparent with dipping reflections	Surface	2. Lat.	Bentley and Anderson, 1998; Ó Cofaigh et al., 2002, 2005a, 2008; Jamieson et al., 2012
89.	Marguerite Trough	Mid-shelf				Surface	2. Lat.	Ó Cofaigh et al., 2005a; Jamieson et al., 2012
90.	Marguerite Trough	Mid-shelf				Surface	2. Lat.	Ó Cofaigh et al., 2005a;

									Jamieson et al., 2012
91.	Marguerite Trough	Mid-shelf					Surface	2. Lat.	Ó Cofaigh et al., 2005a; Jamieson et al., 2012
92.	Marguerite Trough	Mid-shelf					Surface	2. Lat.	Ó Cofaigh et al., 2005a; Jamieson et al., 2012
93.	Marguerite Trough	Mid-shelf					Surface	2. Lat.	Ó Cofaigh et al., 2005a; Jamieson et al., 2012
94.	Marguerite Trough	Inner-shelf					Surface	2. Lat.	Ó Cofaigh et al., 2005a; Jamieson et al., 2012
95.	Marguerite Trough						Surface		Livingstone et al., 2013
96.	Marguerite Trough						Surface		Livingstone et al., 2013
97.	Marguerite Trough						Surface		Livingstone et al., 2013
98.	Marguerite Trough						Surface		Livingstone et al., 2013
West Antarctic margin									
99.	Belgica Trough	Inner-shelf	40		20	Transparent with dipping reflections	Surface		Ó Cofaigh et al., 2005b, 2008
100.	Belgica Trough	Inner-shelf					Surface		Ó Cofaigh et al., 2005b
101.	Belgica Trough	Mid-shelf					Surface		Ó Cofaigh et al., 2005b
102.	Belgica Trough	Mid-shelf					Surface		Ó Cofaigh et al., 2005b
103.	Pine Island Trough East	Outer-shelf			20	Transparent	Surface 16 – 12 ka		Evans et al., 2006; Graham et al., 2010; Kirshner et al., 2012
104.	Pine Island Trough East	Outer-shelf			20		Surface 16 – 12 ka		Graham et al., 2010; Kirshner et al., 2012
105.	Pine Island Trough East	Mid-shelf			15		Surface 16 – 12 ka		Graham et al., 2010; Kirshner et al., 2012
106.	Pine Island Trough East	Mid-shelf	16		35	Prograding layered and chaotic	Surface 16 – 12 ka	1. Vert. & 2. Lat.	Lowe and Anderson, 2002; Graham et al., 2010; Kirshner et al., 2012
107.	Pine Island Trough East	Mid-shelf	22	12	56	Prograding layered and chaotic	Ice retreated before 12.3 cal ka. Took 600-2000 yrs to form	1. Vert. & 2. Lat.	Lowe and Anderson, 2002; Evans et al., 2006; Graham et al., 2010; Kirshner et al., 2012
108.	Pine Island Trough West	Outer-shelf	20		60	Transparent	Buried		Gohl et al., 2013

109.	Pine Island Trough West	Outer-shelf	8			Transparent	Surface		Gohl et al., 2013
110.	Pine Island Trough West	Outer-shelf	10		60	Transparent	Buried		Gohl et al., 2013
111.	Getz-Dotson Trough	Middle-shelf	20			Transparent	Surface		Graham et al., 2009; Smith et al., 2011; Gohl et al., 2013
112.	Getz-Dotson Trough	Inner-shelf	25			Transparent	Surface		Graham et al., 2009; Smith et al., 2011; Gohl et al., 2013
113.	Unnamed Trough off Hobbs coast	Mid-shelf	18	8	80	Transparent	Surface		Klages et al., 2014
114.	Eastern Basin Trough 6	Inner-shelf					Surface		Mosola and Anderson, 2006
115.	Eastern Basin Trough 6	Inner-shelf					Surface		Mosola and Anderson, 2006
116.	Eastern Basin Trough 6	Outer-most shelf					Surface	3. Outer-most shelf	Mosola and Anderson, 2006
117.	Eastern Basin Trough 5	Inner-shelf					Surface		Mosola and Anderson, 2006
118.	Eastern Basin Trough 5	Mid-shelf					Surface Composite?		Mosola and Anderson, 2006
119.	Eastern Basin Trough 5	Outer-most shelf					Surface		Mosola and Anderson, 2006
120.	Eastern Basin Trough 4	Mid-shelf	30				Surface		Bart, 2004; Mosola and Anderson, 2006; Bart and Owolana, 2012
121.	Eastern Basin Trough 4	Mid-shelf	140	100	80	Chaotic with seaward dipping reflections	Surface		Bart, 2004; Mosola and Anderson, 2006; Bart and Owolana, 2012
122.	Eastern Basin Trough 4	Outer-shelf	30				Surface/ partially-buried		Bart, 2004; Mosola and Anderson, 2006; Bart and Owolana, 2012
123.	Eastern Basin Trough 4	Outer-shelf					Surface/ partially-buried		Bart, 2004; Mosola and Anderson, 2006; Bart and Owolana, 2012
124.	Eastern Basin Trough 4	Outer-most shelf					Surface	3. Outer-most shelf	Bart and Owolana, 2012
125.	Eastern	Inner-	100		25	Chaotic	Surface		Howat and

	Basin Trough 3	middle shelf							Domack, 2003; Mosola and Anderson, 2006
126.	Eastern Basin Trough 3	Outer-most shelf					Surface	3. Outer-most shelf	Howat and Domack, 2003; Mosola and Anderson, 2006
127.	JOIDES Central trough	Mid-shelf	40		80	Concave-down reflections that dip seaward	Surface		Anderson and Bartek, 1992; Anderson et al., 1992; Shipp and Anderson, 1997; Shipp et al., 1999
128.	Drygalski Trough	Several wedges on middle-shelf	70 (largest wedge)				Surface		Shipp et al., 1999
129.	Drygalski Trough	Inner-shelf					Surface		Greenwood et al., 2012
130.	Trough extending from Mackay glacier	Several wedges on inner-shelf					Surface		Greenwood et al., 2012
East Antarctic margin									
131.	Mertz Trough	Mid-shelf		30	80		Surface		McMullen et al., 2006
132.	Mertz Trough	Mid-shelf		30	80		Surface		McMullen et al., 2006
133.	Prydz Channel/ Nella Rim	Inner-shelf					Surface		Domack et al., 1998; O'Brien et al., 1999
134.	Prydz Channel west	Mid-shelf			300	Dipping internal reflections	Surface Composite?		Domack et al., 1998; O'Brien et al., 1999
135.	Prydz Channel west	Mid-shelf					Surface		Domack et al., 1998; O'Brien et al., 1999
136.	Prydz Channel west	Mid-shelf					Surface		Domack et al., 1998; O'Brien et al., 1999
137.	Prydz Channel east	Mid-shelf	20		50	Transparent with dipping reflections	Surface		Domack et al., 1998; O'Brien et al., 1999
138.	Prydz Channel east	Mid-shelf					Surface		Domack et al., 1998; O'Brien et al., 1999
139.	Prydz Channel – Lambert Deep	Mid-shelf	5		10 - 30		Surface		Domack et al., 1998; O'Brien et al., 1999
140.	Prydz Channel – Lambert Deep	Inner-shelf					Surface		Domack et al., 1998; O'Brien et al., 1999
141.	Nielsen Basin Trough	Outer-shelf					Surface		Mackintosh et al., 2011

142.	Iceberg Alley Trough	Outer-shelf		Surface	Mackintosh et al., 2011
143.	Iceberg Alley Trough	Outer-shelf		Surface	Mackintosh et al., 2011

Highlights

We present an inventory of 143 high-latitude grounding-zone wedges

Grounding-zone wedges are typically less than 15 km long and 15 to 100 m thick

Fast ice-streaming flow is probably necessary for grounding-zone wedge formation

Ice shelves force wedge formation by restricting vertical accommodation space

Continental shelf geometry can control the position of still-stands in the ice margin